



Helpful Undergarment for Getting rid of Stress

Final Project Report
Submitted April 30, 2018
MEAM 445/446, MEAM Senior Design
September 2017 - April 2018

Team 09: pennhugs@gmail.com
Becky Abramowitz - rabram@seas.upenn.edu
Matt Caltabiano - mcaltab@seas.upenn.edu
Anna Estep - annaest@seas.upenn.edu
Erica Higa - ehiga@seas.upenn.edu
John Killoran - jkill@seas.upenn.edu
Sean Trahan - trahanse@seas.upenn.edu

Faculty Advisor:
Dr. Jennifer R. Lukes, Professor, MEAM
jrlukes@seas.upenn.edu

Technical Advisors:
Dr. Michael Carchidi, Professor, MEAM
carchidi@seas.upenn.edu
Dr. Daniel Bogen, Retired Professor, BE
dan@seas.upenn.edu

Abstract

One in 68 children have an Autism Spectrum Disorder which is often accompanied by sensory sensitivities and a tendency to become overwhelmed and panicked when overstimulated [1]. Deep Pressure Therapy can help reduce feelings of panic and stress by triggering the release of serotonin and dopamine [2]. Existing Deep Pressure Therapy mechanisms are bulky, non-transportable, and/or difficult to use. HUGS is a customizable, inflatable undergarment controlled by a mobile application that proactively provides deep pressure to the user in response to biometric and environmental signs of overstimulation.

Testing on moisture and comfort informed material selection, COMSOL and mathematical models yielded the optimal system geometry, and 20 pressure sensors analyzed the uniformity of applied pressure. Targeting children aged four to six, HUGS weighs 0.34 kilograms, lasts 14+ hours between charges, and applies a force of 0 to 19.5% percent of the user's body weight. The HUGS garment outperforms existing deep pressure therapy solutions by applying more uniform pressure and proactively activating in response to internal and external stimuli.

Future work on HUGS would include scaling the manufacturing process to create a replicable and marketable product as well as integrating a machine learning algorithm to predict sensory overload.

Team HUGS is comprised of Anna Estep, Becky Abramowitz, Erica Higa, John Killoran, Matt Caltabiano, and Sean Trahan and is advised by Dr. Jennifer Lukes.

Table of Contents

Abstract	1
Table of Contents	2
1 Executive Summary	5
2 Statement of Roles and External Contributions	6
3 Background	8
3.1 Background on Autism Spectrum Disorder	8
3.2 Existing Solutions	10
3.3 Identified Opportunity	11
4 Objectives	11
4.1 Design Impact of Standards	13
4.1.1 Flammability	13
4.1.2 FDA General Wellness Products	13
4.1.3 Consumer Product Safety Act	14
4.1.4 Bluetooth Certification	14
4.1.5 IRB Testing	15
5 Design and Realization	15
5.1 Design Down Selection	15
5.1.1 Initial Down Selection	15
5.1.1.1 Inflatable Filling Subsystem	19
5.1.1.2 Inflatables Design	20
5.1.1.2 Characterization and Down-Selection of Mechanical Subsystems	20
5.1.2 Inflatable Belt Prototype	22
5.1.2.1 Heat Transfer Model	23
5.1.2.2 Design	24
5.1.2.3 Manufacturing	24
5.1.3 Compression Belt Prototype	24
5.1.3.1 Material Analysis	24
5.1.3.2 Design	25
5.1.3.3 Manufacturing	26
5.1.4 Secondary Design Down Selection	27
5.2 Mechanical	28
5.2.1 Material Selection	28
5.2.1.1 Material Selection for Absorptivity	28
5.2.1.2 Material Selection for Comfort	30
5.2.1.3 Overall Material Selection	31
5.2.2 Bladder Geometry	31
5.2.2.1 Stiffness Analysis for Bladder Geometry	32
5.2.2.2 Effect of Bladder Size on Heat and Mass Transfer	33
5.2.2.3 Effect of Bladder Size on Perceived Heat	33
5.2.2.4 Effect of Bladder Size on Perceived Uniformity	34
5.2.2.5 Bladder Geometry Selection	35

5.2.3 Manufacturing	36
5.2.3.1 Bladders	36
5.2.3.2 Inner Material	39
5.2.3.3 Outer Material	39
5.3 Hardware, Software	40
5.3.1 Sensor Selection	40
5.3.2 System Architecture	40
5.3.3 Communication and Data Storage	42
5.3.4 Microcontroller and Battery Selection	42
5.3.5 Electrical System	43
5.3.6 Sensor Calibration	46
5.3.7 Embedded Software System	47
5.3.8 Mobile Application	48
5.4 Final System Embodiment and Function of HUGS	49
5.4.1 Manufactured Final Version	50
5.4.2 Layers	50
5.4.3 Washability	50
5.4.4 Variable Size	50
6 Validation and Testing	51
6.1 Human Testing	51
6.2 Pressure Distribution Testing	51
6.2.1 Pressure Distribution Test Setup	51
6.2.2 Pressure Distribution Results	53
6.3 Comfort Test	54
6.4 Sensor Testing	55
6.5 Maximum Force Applied	56
6.6 Inflation Time	57
6.7 Weight	57
6.8 Battery Life	57
6.9 Noise at 1m	58
6.10 Response Time	58
7 Discussion	59
7.1 Target Versus Accomplished Performance	59
7.2 Recommendations	61
8 Budget, Donations, and Resources	62
9 Intellectual Property	63
References	64
Appendix	67
Summary of Feedback from Experts	67
Microcontroller Source Code	68
global.h	68
main.cpp	69

Pressure Distribution Testing Source Code	72
PressureSensor.m	72
pressureMap.m	73
Pressure Distribution MATLAB Outputs	75
Squeeze Jacket	75
HUGS	75
Patents on Similar Products and Designs	76
Rayleigh Number and Perceived Heat MatLab Code	77
Heat Transfer MatLab Code	78

1 Executive Summary

Autism Spectrum Disorder is a condition that impairs a person's ability to communicate effectively and can range in severity. People who have ASD are susceptible to sensory overload, in which all sensory inputs are magnified, and the amount of information is too much for the brain to handle. [This video](#) is a good simulation of a sensory overload event [3]. Clearly, this event is very jarring and anxiety inducing. One of the most effective ways to deal with sensory overload is Deep Pressure Therapy (DPT) during or after the episode. Deep Pressure Therapy is an application of pressure to the body that is meant to mimic the pressure from a hug since hugs are typically calming but, for some people with ASD, physical contact can contribute to further anxiety. Adults with ASD are more likely to identify when this event is about to occur and apply the therapy themselves or remove themselves from the hostile environment, but children are too young to understand what is happening and do not have the autonomy to move somewhere else or react properly to the situation.

The Helpful Undergarment for Getting rid of Stress (HUGS) is a wearable for children that applies Deep Pressure Therapy to the wearer during these sensory overload events. It also uses environmental sensors (light, sound, temperature, and accelerometer) and a heart rate sensor to predict when the user is in a potentially hostile environment and a sensory overload event may occur. Two prototypes were pursued in the fall: an inflatable system that uses air bladders filled using a pump to apply pressure and a rotating shaft system that tightens belts around the body to apply pressure. One of the most important metrics for testing these two prototypes was pressure distribution. According to feedback from consulted occupational therapists (Appendix Table A1), a uniform pressure distribution is essential to DPT since non-uniformities can add to further anxiety. At the end of the fall semester, we tested the pressure distribution for both devices and found that the inflatable device had a more uniform distribution. A force analysis of the rotating system performed with Dr. Michael Carchidi also verified that it is not possible to get a uniform distribution and the inflatable system was chosen.

In the spring semester, the team focused on manufacturing the full device, creating the app that controls the device, and performing tests to validate the system's design choices, sensor response, and, most importantly, pressure distribution. We used a butane soldering iron to seal, or effectively melt, vinyl sheets together for the inflatable belts. The belts were then sewn into a polyester inner material and a nylon mesh outer material. Once the system was completed we tested the pressure distribution against an existing DPT device, Squeeze, and found that our device's pressure distribution was more uniform than Squeeze's. Lastly, we tested our sensors and the device activated when any of the threshold values were passed. Through these validation tests, HUGS has proven to be a novel idea that has the potential to help children with ASD with their sensory overload attacks.

2 Statement of Roles and External Contributions

Becky Abramowitz: Becky was primarily in charge of the software development and electrical integration of the system. She designed the mobile application, built the pressure sensor testing set-up, and wrote the onboard code. She was instrumental in selecting the microcontroller and biometric and environmental sensors. Becky filtered the pressure sensor data, calibrated the biometric and environmental sensors, and configured HUGS to communicate with the mobile app via Bluetooth. In the first semester, Becky was on the compression belt prototype sub-team, researching motors, configuring the motor driver, and developing the test setup.

Matt Caltabiano: Matt was primarily in charge of constructing the logistics of the Senior Design team. He was instrumental in creating the presentations used in the second semester. He built the poster and pamphlet used on Design Day. He was in charge of communications with advisors and third parties, such as Dr. Jennifer Lukes and Dr. Daniel Bogen--with whom he met to determine which sensors to use. He performed the sweat-wicking test, compiling and analyzing the data afterward. In the first semester, Matt was on the inflatable belt sub-team, researching pumps, IRB approval, and material selection.

Anna Estep: Anna was primarily in charge of optimizing the heat and mass transfer of the system, by determining the system's optimal geometry. She was instrumental in material testing and selection using both empirical tests, and models created in MATLAB and COMSOL. She conducted the moisture wicking, sweat-wicking, and comfort tests. She also conducted the two-point touch test to map the optimal spacing between the bladders. She was in contact with Dr. Lukes for help in determining system geometry. Anna was in charge of all purchasing with TBO. During the first semester, Anna was on the compression belt sub-team, receiving MTS training and using stress-strain data on materials she selected to construct the prototype.

Erica Higa: Erica was primarily in charge of the manufacturing of the physical system including system design and integration. Additionally, she developed the heat and moisture testing procedures, performed the moisture and sweat-wicking tests, and met with Dr. Bogen to determine which sensors to use. She constructed the full-scale prototypes used for testing and design day, improving on the manufacturing process throughout the year. Additionally, she aided in creating the slide decks for presentations and submitting Tasks and Salaries each week. In the first semester, Erica was on the inflatable belt sub-team working on models for heat transfer of the system, as well as manufacturing the initial prototype used on the test set-up.

John Killoran: John was primarily involved with developing the electronics of the system and coordinating the inflation and deflation of the inflatables, as well as the wiring, amplification, and filtering of the sensors. He read through documentation on temperature, heat, photo, and noise sensors in order to understand the promise of incorporating them into the final design. He collected real-time data on himself for temperature, sound, heart-rate, and light sensors, and compiled the data. He integrated the internal pressure sensor into the system and validated the functionality of all the sensors. In the first semester, John was on the inflatable belt sub-team working on the heat transfer model, choosing pumps, and creating the test set-up.

Sean Trahan: Sean was primarily in charge of optimizing the heat and mass transfer of the system, by determining the system's optimal geometry. As well, he developed a COMSOL pressure distribution and stress analysis model, developed heat and moisture transfer test procedures, and conducted the two-point touch test to map the optimal spacing between the bladders. He was in contact with Dr. Lukes for help in determining system geometry. He conducted the comfort testing and created a MATLAB model to determine the heat transfer of the system. In the first semester, Sean was on the compression belt sub-team, printing the shafts for the prototype and working closely with Dr. Carchidi to model the pressure distribution around the elliptical torso.

Dr. Jennifer Lukes: Dr. Lukes is Mechanical Engineering professor at the University of Pennsylvania and was the primary technical advisor for the team, providing insight on the heat conductivity properties of the materials of the system, as well as general advice for completing the project successfully.

Dr. Daniel Bogen: Dr. Bogen is retired Bioengineering professor at the University of Pennsylvania and was a technical adviser to the team, providing insight on the functionality and feasibility of various biometric and environmental sensors used on the device.

Dr. Michael Carchidi: Dr. Carchidi is Mechanical Engineering professor at the University of Pennsylvania and was a technical adviser to the team providing insight on the feasibility of compression belts providing uniform pressure to an elliptical cross section.

Dr. Bruce Kothmann: Dr. Kothmann is Mechanical Engineering Senior Lecturer at the University of Pennsylvania and was a technical adviser to the team providing insight on the stiffness analysis for the bladder geometry.

Robert "Wes" Thomas: Wes is Robotics masters student at the University of Pennsylvania and was the teaching assistant assigned to the team, providing general project feedback and technical advice throughout the duration of the project.

Dr. Graham Wabiszewski: Dr. Wabiszewski is a Mechanical Engineering professor at the University of Pennsylvania and was instrumental in approving the additional funding necessary for the team to procure an existing solution for testing. He also provided feedback on design decisions and presentations, as well as technical advice throughout the project.

MATLAB: MATLAB was leveraged to create heat transfer models used in determining the optimal system geometry.

COMSOL: COMSOL was leveraged to create pressure distribution and stress analysis simulations used in determining the optimal system geometry.

3 Background

The following section provides background on Autism Spectrum Disorder and the use of Deep Pressure Therapy to alleviate the negative side-effects of stress and sensory overload. While there are existing Deep Pressure Therapy solutions, the HUGS device fills a currently unimplemented niche of design specifically for the needs of young children.

3.1 Background on Autism Spectrum Disorder

The rate at which people in the United States are diagnosed with an Autism Spectrum Disorder, hereafter ASD, has been on the rise for decades [4]. While these disorders cover a wide range of symptoms, commonalities among most disorders include impaired communication skills, social deficits, and atypical responses to sensory information. In fact, 96% of children with ASD report an abnormal response to sensory input [5]. This hyper- or hypo- sensitivity causes behavioral problems for children with ASD and is often the target of therapeutic intervention.

Hypersensitivity in particular can cause children to become overwhelmed by the various stimuli in their environment. Jon Coleman, an 18-year-old with ASD, describes this hypersensitivity, "The things around you are kind of overwhelming. So, it could be like an electric light flickering or a sound of squeaky shoes on tile or something like that, and that can overwhelm you" [6]. He describes auditory and visual hypersensitivities, but children with ASD can have sensitivities to any or all of the senses. Jon also points out how overwhelming this hypersensitivity is; this feeling of being inundated with sensory information can cause meltdowns and, in more severe cases, self-harming behaviors in children with ASD [5].

There are various treatment options for hypersensitivity, but one of the most common therapies is Deep Pressure Therapy, or DPT. Deep pressure is the application of firm pressure over all or part of the body and is used for children with ASD to calm the effects of sensory overload. When used for therapeutic purposes, deep pressure can be administered in a variety of ways including weighted vests and blankets, pressure vests, and hug/squeeze machines. Appendix Table A1 summarizes the important information gained from speaking with experts, all of whom indicated that they used DPT with their patients. Additionally, in a survey sent to parents of children with ASD, 88.3% of parents (n=20) responded that their child had used at least one type of DPT. Due to the wide range of symptoms and needs of children with ASD, clinical studies of DPT are limited. However, there are multiple studies that support DPT as a beneficial therapy. For example, Bestbier and Williams found:

Deep pressure benefits most participants to a statistically significant degree. The variability in individual responses indicates that deep pressure should be tailored to the individual needs of the recipient. Deep pressure seems to have benefits in many areas for most people, but individual responses must be considered in the design of future research [7].

Additional research includes Edelson, et. al., whose, "Preliminary findings support the hypothesis that deep pressure may have a calming effect for persons with autism, especially those with high levels of arousal or anxiety", and Reynolds, et. al., who concluded that "deep pressure stimulation is capable of eliciting changes in autonomic arousal and may be a useful modality in diagnostic groups seen by occupational therapy practitioners" [8] [9]. Thus, DPT is clearly an accepted and widely used therapy for children with ASD.

The success of DPT is dependent on the method of administration and requires uniform pressure across a large surface area, such as the chest, torso, or lap. Two experts, Lisa Russell and Sarah Bujno, both asserted that non-uniform DPT would be less effective or even cause the crisis to worsen. While there are currently no published studies that quantify the performance of uniform DPT, all of the studies that concluded DPT provides positive outcomes for children with ASD used items that are known to administer somewhat uniform pressure (e.g. hug machine, weighted vest) [7] [8] [9]. In order to evaluate what uniform pressure entails, we purchased and tested a hand-pumped inflatable vest from the current market. Acceptable values of pressure variation will be determined from this data, as these vests are commonly used and are known to provide beneficial pressure.

Another important distinction in the application of DPT is continuous versus intermittent pressure application. According to consulted occupational therapists, DPT is most effective when applied for a short time, usually 10-15 minutes, and then removed. This is due to a natural phenomenon known as sensory adaptation, defined by the Oxford Dictionary of Psychology as, "a temporary reduction in the responsiveness of a sensory receptor other than a pain receptor as a result of repeated or continuous stimulation" [10]. When a new stimulus occurs, the brain must determine whether it is a threat. Once the brain has processed that the stimulus is not harmful, sensory adaptation occurs and the sensory receptor decreases response to the constant stimulus [11]. Figure 3.1 shows examples of sensory adaptation in (a) olfactory receptors and (b) retinal photoreceptors [12].

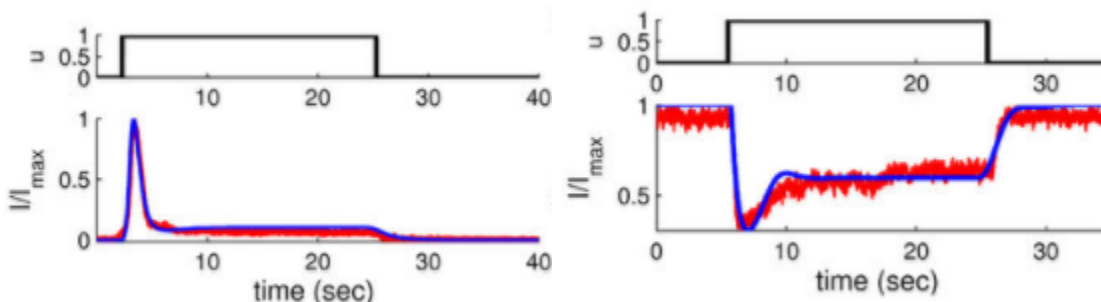


Figure 3.1: (a) Olfactory Sensory Adaptation

(b) Sensory Adaptation in Photoreceptors

The top graph in both (a) and (b) of Figure 3.1 shows the continuous stimuli, applied for 24s and 20s respectively. The bottom graph shows the normalized response of the neurons before, during, and after the applied stimuli. In both cases, the neurons respond to the stimulus, then quickly even out to a lower response level. Although the time scale and degree to which the neuron adapts in these figures may not be directly relatable to humans, as the study was

conducted on salamanders, they do clearly demonstrate the basic concept of sensory adaptation. Additionally, research shows that sensory adaptation occurs in somatosensory neurons [13]. Somatosensory neurons sense conscious perception of touch, pressure, pain, temperature, position, movement, and vibration. These neurons respond to DPT, so it follows that DPT must be applied intermittently in order to be as effective as possible.

3.2 Existing Solutions

On October 19th, 2001, Portia Iversen filed a patent for a “Pressure vest for treating autism” [14]. The pressure vest “comprises a torso-engaging member configured to engage the torso of the wearer” with a sensor to detect moisture levels of the person wearing the vest. The vest would activate in response to detected moisture. Thus, the idea of using DPT to calm children with ASD is not novel. There are many versions of existing solutions for this problem.

The simplest and least expensive of these solutions is a compression shirt that is a few sizes too small. While it succeeds in applying generally uniform pressure for the child, the process of putting on the shirt is difficult, and the child quickly adapts to the pressure due to sensory adaptation.

Another DPT solution is the use of a weighted vest or blanket, such as the South Paw Bear Hug or the Snug-N-Hug [15] [16]. Although it is slightly more expensive than the compression shirt, the weighted vest is easier for children with ASD to use. It allows for a greater amount of pressure to be applied, however the pressure applied is only in one direction due to gravity. Having established the advantages of uniform pressure, this proves this solution to be suboptimal. Additionally, due to sensory adaptation, the child quickly adapts to the pressure applied by the vest and it must therefore be taken on and off repeatedly to benefit the child.

The two most robust solutions currently available are: (1) a hug machine and (2) versions of a deep pressure vest, particularly Squeeze, T-Jacket, Snug Vest, and BioHug [17] [18] [19] [20]. The hug machine, first invented by Temple Grandin, is a large box with two padded sides, which compress together to apply lateral pressure to the user. The machine is at least double the size of the user, which makes it costly and non-transportable [21]. Because it is bulky, difficult to transport, and expensive, it does not serve as a practical solution for children with ASD.

There are two current versions of the deep pressure vest: (1) hand-pumped and (2) motor-pumped. Squeeze, the hand pumped vest, is compact and able to be worn under loose jackets and other garments, but must be worn over an undershirt [17]. Additionally, the user must directly apply the pressure by his/herself. The T-Jacket, a deep pressure vest which costs ~\$600, solves this as it actively applies pressure using a motorized pump, however, it does so at the cost of size. It is bulkier than Squeeze and non-discrete which draws unnecessary attention to the user.

Furthermore, the aforementioned solutions fail to actively sense when a child is having a period of high anxiety and respond to it. Thus, there is significant room for innovation within this design space.

3.3 Identified Opportunity

None of the existing solutions were designed for those who are unable to predict sensory overload or apply the therapy autonomously. HUGS will target children between the ages of four and six who are higher functioning on the Autism spectrum. Since the median age of ASD diagnosis is 3 years, 10 months [1], this is a present yet underserved demographic, and need for a product in this category has been validated by conversations with multiple occupational therapists and experts. To ensure autonomy and mitigate burden on the caregiver, HUGS will react to changes in the child's biometric data and apply preemptive deep pressure automatically. Since children in this age range are usually accompanied by a caregiver, HUGS must also be able to be controlled remotely; the device will have an accompanying software platform to receive timely data from and provide commands to the HUGS device. To ensure comfort, HUGS must weigh less than a kilogram, and since children in this age range are active and often enrolled in day time programs, HUGS must have a battery life that lasts throughout the day, approximately ten hours.

4 Objectives

The following section details the technical objectives of the HUGS device as well as the rationale behind these guidelines.

Table 4.1: Key Target Specifications for HUGS Device

Objective	Target Specification
Pressure Distribution	Uniform (defined below)
Max Force Applied	15.0% of body weight
Inflation Time	20 seconds
Response Time	5.0 seconds
Battery Life	10 hours
Noise at 1 meter	50 db
Weight	<0.80 kg

The HUGS device's main objective was to proactively provide deep pressure therapy to the user in response to stimuli in a safe manner. Shown in the table above, there were seven key target specifications the team set out to achieve.

The first goal was to achieve a uniform pressure distribution as the team was informed by experts—Lisa Russell and Sarah Bujno—that a non-uniform distribution would be less effective or even cause the crisis to worsen. To do this, the team set out to achieve a pressure distribution at least as uniform as an existing solution on the market. This existing solution was Squeeze. Once the team had the final pressure distribution test setup, the standard deviation of pressures of the Squeeze device was calculated to be 7.95 kPa.

The desired applied pressure was based on studies by Temple Grandin in which forces were applied laterally to the torso of children under 8-9 years old [21]. Converting these forces to uniform pressure supplied around the child's torso yielded pressures of up to 10.0 - 15.0% of a standard four to six-year old child's body weight which could be safely applied to a child to produce a desirable state. This was validated further by other similar deep pressure therapy experiments related to weighted vests by Buckle et al. [22], and other deep pressure therapy products on the market. Although the goal range of supplied pressures was higher in Grandin's Hug Machine than even the peak pressure supplied by even the heaviest of weighted vests sold, it was vital for the system to be able to achieve the high peak pressures that Grandin was able to supply because HUGS would need to be as effective as possible over short bursts of time, including scenarios in which the sensory input from a child might call for higher pressure.

The response and settling times were selected to minimize the impact of an average length episode within physical reason. Sensory overload episodes in children can reach maximum degree of symptoms within minutes and are followed by states of increased anxiety for periods of time ranging from seconds to half an hour [23]. Furthermore, symptoms of on-setting states of stress can become evident well before the maximum degree of stress begins. Since the system would be running a continuous loop, it was reasonable to assume that the sensors would react quickly to change, though the minimum actuation threshold would likely not be instantaneously reached, leading to a response time of five seconds. The pressure-application components would have a greater constraint on time of actuation as they require physical manipulation and moving parts. While the time to achieve a steady-state pressure should be within the onset of an attack, there must be some delay to prevent any shock or uptick in anxiety from the child not being able to process his or her change in state. This tradeoff informed the goal of a twenty second settling time.

The device needs to be able to run continuously throughout the day, so the parent or guardian would not have to charge it and thus yield it ineffective while it is needed. As a result, the target battery life was 10 hours, allowing the device to be put on at 8:00 AM and operate until 6:00 PM. This gives room on either side of the wearable hours for the child to be without the device when waking up in the morning or going to bed at night.

It is also important that the device is sufficiently quiet that it does not disturb the child's daily activity or provide unnecessary sensory input to the child. As a result, the targeted level of sound at 1 meter was 50 decibels, which is equivalent to a quiet conversation at home [24].

Finally, the mass of the device needed to be restricted to ensure both comfort and inconspicuousness. This limitation was corroborated by all consulted authorities with

experience with autistic children and deep pressure therapy. A standard weighted vest is often around 2.5 kilograms but is considered to be “too much for [younger] children” and is often accompanied by a social stigma. Designing a lighter and smaller vest increases the comfort during non-actuated use and aids in device aesthetics. Based on light-weight deep pressure therapy products like the T-Jacket and Squeeze vests, the targeted specification was 0.80 kg [17] [18]. While heavier than the devices lightweight counterparts, this is still significantly lighter than any weighted jacket.

4.1 Design Impact of Standards

There are five regulatory standards by which HUGS must abide: CFR flammability guidelines, FDA general wellness standards, the Consumer Product Safety Act, Bluetooth guidelines, and IRB approval.

4.1.1 Flammability

The Code of Federal Regulations (CFR) defines standards for the types of wearables that can be produced and sold. Title 16, Part 1610 of the CFR indicates that textiles used in wearables must be tested and classified into either Class 1, 2, or 3 in increasing order of flammability [25]. Certain fabrics, including acrylic, modacrylic, nylon, olefin, polyester, wool, and plain surface fabrics weighing at least 2.6 ounces per square yard have been consistently shown to meet CFR standards and are exempt from testing. To ensure that the device complies with CFR standards, materials first considered for use in the undergarment were from the list of exempt materials above. The textiles used in the final product were polyester and nylon, both of which are exempt materials.

Per the Flammable Fabrics Act vinyl plastic film is a regulated fabric. Title 16 Part 1611 of the CFR indicates the standard for the flammability of vinyl plastic film, the material used for the inflatable bladders. Section 4(a) of the act states that “in determining whether an article of wearing apparel is so highly flammable as to be dangerous when worn by individuals, only the uncovered or exposed part of such article of wearing apparel shall be tested” [26].

Since the vinyl used in the device is neither uncovered nor exposed, the product meets CFR standards.

4.1.2 FDA General Wellness Products

The FDA declared in July 2016 that “general wellness products” are exempt from their regulations so long as they are intended for general wellness and are considered low-risk [25]. Compliant products must reduce the impact of certain chronic conditions, specifically those that are positively affected by healthy lifestyle choices. The team determined that HUGS would meet these criteria. When classifying the condition as sensory overload episodes, HUGS does satisfy the guideline of reducing the impact of a certain chronic condition where it is understood and accepted that healthy lifestyle choices are an important factor in the outcome of the condition.

4.1.3 Consumer Product Safety Act

There are additionally various consumer electronics certifications required to bring HUGS to market. While HUGS was not brought to market during the Senior Design time frame, the team considered the requirements should HUGS ever be brought market. It would need to abide by the Consumer Product Safety Act of the United States Consumer Product Safety Commission.

Applicable regulations include testing the product by an independent third-party laboratory because HUGS is a children's product [27]. Testing would abide to Title 16 Part 1107, mandating that continued testing of the product be performed periodically and upon a material change in the product. It also indicates labeling requirements should the product ever be brought to market. Furthermore, the device needs to abide to Title 16 Part 1109, pursuant to component part testing and certification.

Ultimately, given the scope of Senior Design, the team did not test the product for its adherence to the Consumer Product Safety Act or the Consumer Product Safety Improvement Act. However, given that adherence to this act in the design of the product was considered, the team expects that upon review of the device, the final product would be certified by the United States Consumer Product Safety Commission.

4.1.4 Bluetooth Certification

Given that the device uses Bluetooth to communicate with the mobile application, it would need to comply with Federal Communications Commission regulations to be sold in the United States and would need to be Bluetooth qualified.

To be Bluetooth qualified, "conformance must be verified, an IP license must be granted, and logo and wordmark usage rights need to be received along with verified interoperability" [28]. To verify radio conformance, radio testing would need to be performed at a Bluetooth-qualified testing facility and Qualified Design Identification would need to be obtained. Furthermore, the Bluetooth stack's conformance to the Bluetooth specification would need to be verified. Finally, the product would need to be listed in the Bluetooth SIG end product listing, incurring a cost of \$8000.

To be certified by the FCC, the device would need to abide by Part 15 of Title 46 of the FCC. To operate in the 2400 - 2483.5 MHz band, the device must meet either Part 15.247, being limited to frequency hopping and digitally modulated schemes, or Part 15.249, not imposing restriction on either the modulation scheme or the end application.

Other standards to be tested might include, Part 15.207, conducted emission test, Part 15.209, spurious emissions test, and Part 15.203, antenna requirements test.

It is expected that the device pass FCC certification.

4.1.5 IRB Testing

Under FDA regulations, an Institutional Review Board, hereafter IRB, would need to approve any tests conducted with the device, since it would be classified as biomedical research involving human subjects.

The team attended a training session on obtaining IRB approval at the University of Pennsylvania using the Human Subject Electronic Research Application. Given the scope of the project, as well as resources provided, the team decided to not pursue approval in the scope of Senior Design. Should the device be eventually brought to market, however, IRB approval would be required to determine the validity of the device.

5 Design and Realization

The following section details the design process for the HUGS device, beginning with the initial down selection process, then following the initial prototyping efforts on two unique designs. This section also includes the design decisions in the final HUGS garment as well as the manufacturing techniques used in product realization.

5.1 Design Down Selection

The HUGS design down-selection process began with an initial down-selection step which narrowed from a broad range of design ideas to two designs. These designs were then prototyped, and further down selected. This process is detailed below.

5.1.1 Initial Down Selection

There are four categories of existing solutions used to apply DPT, as shown in **Table 5.1**.

Table 5.1: Existing Deep Pressure Therapy Products

(a) Hug Machine	(b) Undershirt	(c) Weighted Vest / Blanket	(d) Compression Jacket
[37] 	[38] 	[39], [40] 	[18] 

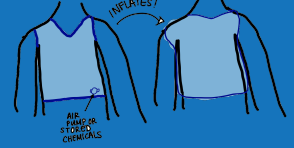
Table 5.1 (a) shows a hug machine. This technology was made famous by Dr. Temple Grandin, who developed a Squeeze Machine for herself in order to experience the benefits of Deep Touch Therapy [21]. While effective, this solution is expensive (~\$3500 per machine), unsuitable for children under eight years old, and nonportable. **Table 5.1 (b)** highlights the inexpensive option

of wearing a thin undershirt, such as a swim shirt that is a size too small. This solution is one that Dr. Trenna Sutcliffe, MD FRCPC FAAP, of Sutcliffe Developmental and Behavioral Pediatrics often uses for children who need extra sensory therapy via deep pressure. While it is inexpensive, safe, and portable, it lacks the necessary intermittency to avoid sensory adaptation. Of 21 surveyed parents, 16 reported that their child with ASD had used either a weighted vest (**Table 5.1 (c)**) or weighted blanket. Like the thin undershirt, the weighted vest shown in **Table 5.1 (c)** is relatively inexpensive (~\$70), safe, and portable, but it also delivers less meaningful therapeutic input over time due to sensory adaptation. The final existing market solution is an inflatable jacket such as the T-Jacket **Table 5.1 (d)**, which is more expensive (~\$600), but portable, safe, and controllable.

Some other potential but unrealistic solutions include an improved hug machine (not portable), a mechanical, huggable teddy bear (not deep pressure therapy), a chemical reaction induced inflatable bladder solution (unsafe for the child), and Non-Newtonian fluid filled bladders that stiffen and harden via vibrations (infeasible/too heavy).

The viable solutions include: a shirt material made of electroactive polymers, a mechanical corset or ratcheting system using springs, tightening belts, pneumatics, or tightening interwoven string technologies to tighten and loosen around the torso, and an inflatable garment making use of either air bladders or expanding veins. These designs were initially assessed qualitatively, as shown in **Table 5.2**.

Table 5.2: Potential Deep Pressure Solutions

	Electroactive Polymers 	Mechanical Corset 	Inflatable Garment 
Price	\$\$\$	\$	\$
Safety	Unknown	Moving Parts	Safe (already used)
Comfort	Comfortable	Mechanical Parts, Stiff, Uncomfortable	Soft, Flexible, Light
Pressure	Uniform	Uniform	Uniform
Aesthetic	Thin, not visible under shirt	Lumpy under shirt	Somewhat thin
Durability	Unknown	Moving parts could break	Leaking potential

The qualitative down-selection process was performed by rating the options on a 1-10 scale according to the following categories:

- Safety: How safe would it be for a child to wear the garment throughout the day? This also includes potential for malfunction, including from water damage, physical damage during child's play, and potential harm to the child such as if he/she fell while wearing it. Safety was weighted the highest of all the categories at 25/100 because the safety of the children is the most important factor. If the product is not safe, then validation cannot be achieved, and the product will fail.
- Project Cost: What is the feasibility of carrying out the project within the \$2400 budget allowed for Senior Design? Project cost was weighted at 20/100 because the project must stay within the allotted budget of \$2400 and because a more expensive solution would be less fit for market.
- Aesthetic: Does it look like an undergarment? Can it be made barely visible underneath a child's regular clothes? The aesthetic appeal was given a 15/100 weighting due to responses from parents conveying that current solutions carry a social stigma, and one of the goals of HUGS is to remove this stigma by creating a discreet undergarment.
- Feasibility: Is this a feasible MEAM Senior Design project? Feasibility was given 15/100 because the team needs to be sure it is possible given time and skill constraints. That being said, the team was careful to ensure that feasibility would not overshadow safety or cost since safety is the primary priority and cost also dictates the feasibility of the project.
- Comfort: Will it be comfortable for the child? Comfort was given a 10/100 because it is important that HUGS be as comfortable as possible, but some existing solutions are somewhat uncomfortable and are still utilized frequently, thus comfort was weighted lower than other categories.
- Portability: Can it easily stay on the child for an entire day? Portability was given a 10/100 because it was already decided that HUGS would be working in that design space. It is therefore important but also slightly redundant.
- Durability: Is the device able to withstand washing, long term usage, and child play? Durability was given a 5/100 because it would be an added bonus if HUGS were washable and could withstand months/years of use, however within the scope of Senior Design time, budget, and manufacturing capabilities, this metric was considered the least important.

Table 5.3 shows the rankings of the previously mentioned systems on the aforementioned categories. These rankings underpinned the initial quantitative down selection process.

Table 5.3: Quantitative Down-Selection using Product Characteristics

	Safety (25%)	Cost (20%)	Aesthetic (15%)	Feasibility (15%)	Comfort (10%)	Portability (10%)	Durability (5%)	Total
Electroactive Polymers	8	1	9	6	8	9	9	6.6
Mechanical Corset	6	7	7	10	6	8	4	7.05
Inflatable Garment	9	9	9	9	8	10	8	8.95

It is evident from **Table 5.3** that the Inflatable Garment is the best solution in terms of the defined criteria. The Electroactive Polymer solution is the least viable, but we lacked sufficient information (primarily pressure distribution results) to rule out the Mechanical Corset solution. For this reason, two prototypes were pursued in the fall semester. Each prototype was a singular horizontal band that was used to test the pressure distribution for the devices. We performed further down selection for the pressure application subsystems for each solution.

5.1.1.1 Characterization and Down-Selection of Inflatable Subsystems

The full design of the inflatable garment includes multiple rings of bladders with a sweat-wicking inner material, and a stiff outer material to make sure inflation is primarily inwards, as shown in **Figure 5.1**. However, in the fall we created a single band due to time constraints and the fact that we only needed a single band to test the pressure distribution.

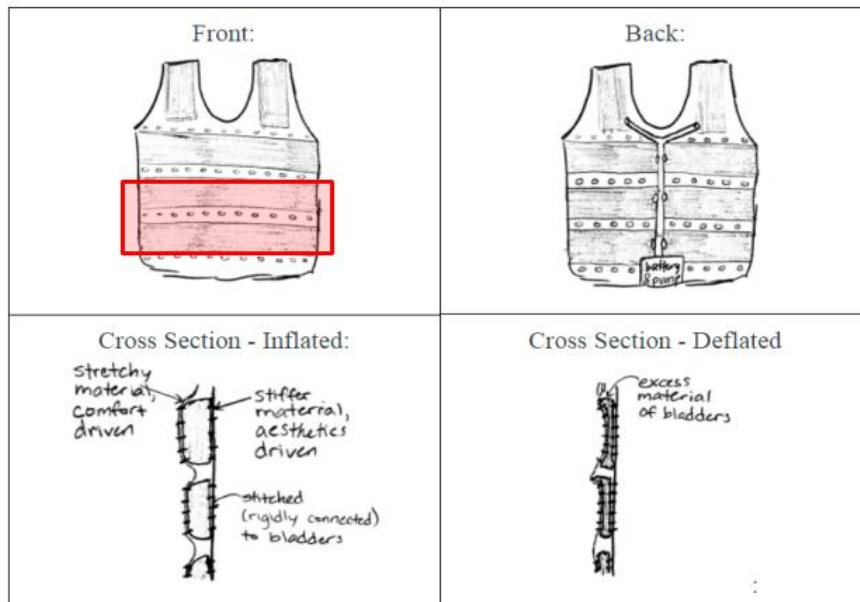


Figure 5.1: Initial Design Sketch of Inflatable Prototype

5.1.1.1.1 Inflatable Filling Subsystem

There are four important factors for determining the mechanism for filling the bladders: (1) safety, (2) the size of the subsystem, (3) the speed with which the bladders fill, and (4) the lifetime of the subsystem. The optimal solution will be safe and minimize the size while maximizing the fill rate and lifetime. The two solutions considered were a chemical reaction which produces gas to fill the bladders and a battery powered pump.

Chemical reactions are appealing because they have a very high fill rate and are compact but unfortunately, they are not reusable and more importantly, they can be dangerous. We looked into several simple chemical reactions. The natural decomposition of hydrogen peroxide produces oxygen, but it is slow and does not produce enough gas [29]. The combination of vinegar and ammonia produces ammonium chloride (a white colored gas) but prolonged exposure to ammonium chloride can cause irritation to the skin, eyes, throat, or lungs [30]. The fermentation of sugar creates carbon dioxide, but ethanol is created as a by-product which is flammable and dangerous to ingest. Other reactions require a lot of reactants or enormous energy input.

The pump solution is less compact than a chemical reaction and, for an appropriately sized pump, has a slower fill rate. However, it has a significantly longer lifetime, since it utilizes a rechargeable battery. The pump is also much safer than the chemical reactions since no flammable or potentially toxic elements are involved.

As a result of the down-selection process in **Table 5.4**, the pump was chosen as the best solution for this subsystem. Both options had high scores for size and they can both be constructed compactly, with slight favor to the chemical reaction method. Additionally, both had moderate scores for fill rate as they can fill the vest quickly given its relatively small size, with again the slight favor to the chemical reaction. The safety and lifetime scores greatly favor the pump because, as noted before, it will utilize a rechargeable battery while the chemical reaction will require cartridge replacements and can be dangerous to have on your body, especially for a child.

Table 5.4: Quantitative Down-Selection of Actuation Method

	Safety (40%)	Size (20%)	Fill Rate (20%)	Lifetime (20%)	Overall
Chemical Reaction	2	8	7	2	4.20
Pump	9	7	5	9	7.80

To help with fill rate, we used two micro pumps placed on either side of the hip so that they wouldn't impede movement of the wearer.

5.1.1.2 Inflatables Design

When considering the design of the inflatables, three design decisions were considered: (1) the orientation of the inflatables, (2) the spacing between each inflatable and (3) the material design of the inflatable.

The team considered two different inflatable orientations: (1) horizontal and (2) vertical. There is no evidence of existing academic research on the advantages or disadvantages of either method. Therefore, the team rationalized that the horizontal orientation would be preferred, for it is the same orientation in which a hug is typically given in person to person interaction; when one individual hugs another the pressure is generally applied horizontally across the torso rather than vertically around the shoulders. Additionally, applying pressure horizontally allows for a complete ring of pressure to be applied, which would enable a more uniform pressure distribution, whereas applying pressure vertically would yield a less symmetric shape.

From a design perspective, the bladders must optimize two engineering constraints: heat dissipation and uniformity. The vinyl bladders on the device act as thermal insulators, meaning that they are poor dissipaters of heat and moisture and the user could easily overheat or feel sticky. We want to maximize heat and mass transfer by strategically arranging spaces of air pockets where the transfer can occur. However, it is important to keep in mind that increasing this gap would have adverse effects on the uniformity of the pressure. If not able to be properly optimized, this could lead to failure of the device in one of the primary design criterium.

Finally, the material design of the bladders and the surrounding material are crucial to the effectiveness of the system. To keep the bladder from expanding away from the torso of the child, an inelastic material was bound to the exterior of the bladder, and a relatively more elastic material—that is comfortable against the body of the user—was used on the interior. Both these materials abide by the regulations discussed in the “Engineering Standards” section and are effective at wicking away heat and sweat from the user. Material analysis for HUGS is discussed further in the Material Selection subsection in the Mechanical section of the paper.

5.1.1.2 Characterization and Down-Selection of Mechanical Subsystems

Mechanically, there are four viable subsystems for compressing a band around the torso: gears, strings, tightening belts, and pneumatics. Due to the wearable size constraint and the non-negligible size for both the actuators and the required compressor, the pneumatic solution was eliminated prior to the down-selection process. **Table 5.5** shows a qualitative comparison of these three solutions. The Ratchet Mechanism solution is gear-based, with tightening bands that contract around the torso when the motor is driven. The Rotational Shaft solution features two rods up the side of the torso, direct-driven by adjacent motors, which tighten a soft belt around the torso as the shaft rotates. The Corset solution has a string interwoven through two sides of a soft material that wraps around a motor shaft to tighten and apply pressure. The designs were assessed on price, safety (quantity and potential hazard of moving parts), comfort, ability to apply uniform pressure, aesthetic, and durability. These fields were consistent with the down-selection criterium used throughout the project and were developed from the problem statement.

Table 5.5: Potential Mechanical Solution Down-Selection

	Ratchet Mechanism	Rotational Shaft	Corset
Price	\$	\$	\$
Safety	Moving parts, could cover to prevent accidents	Moving parts, hand/hair could get wrapped in belts	Fewer moving parts, still potential for hand/hair getting caught
Comfort	Comfort based on number and size of motors	Comfort based on number and size of motors	Fewer stiff/dense parts, stiffer in general
Pressure	More uniform	More uniform	Potentially nonuniform
Aesthetic	Thin, motors may be visible through shirt depending on size	Thin, motors may be visible through shirt depending on size	Thin, one motor on back easily hidden
Durability	Moving parts could break, gears could misalign	Moving parts could break	Wear on the strings, motor could break

From the qualitative down-selection, a quantitative down-selection process led to the selection of a single design. As shown in **Table 5.6**, the categories were given weights based on how well they related to the problem statement and the needs of the project customer. Since the project is for children, safety was deemed to be of the utmost importance, with comfort, aesthetic, and pressure coming in a close second based off of customer feedback and need. Price and durability were ranked at the bottom since it was determined that all the projects could be done under the budget and, as discussed before, durability a reach goal since the project scope focuses mostly on functionality.

Table 5.6: Quantitative Down-Selection of Mechanical Solution

	Safety (25%)	Comfort (20%)	Pressure (20%)	Aesthetic (15%)	Price (10%)	Durability (10%)	Total
Ratchet	6	7	9	5	9	6	6.95
Rotational Shaft	8	8	9	6	9	8	8.00
Corset	7	6	6	8	8	5	6.85

From the down-selection process, the rotational shaft mechanism was selected as the best mechanical implementation. A sketch of a possible final design is shown in **Figure 5.2**.

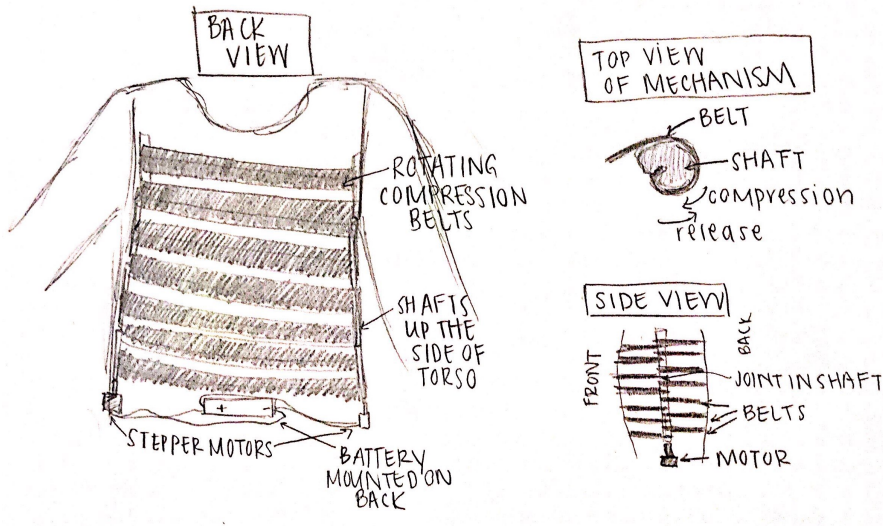


Figure 5.2: Sketch of Ratchet Mechanism Final Design

5.1.2 Inflatable Belt Prototype

A small-scale prototype of the inflatable garment was analyzed and built in order to further down-select between the two most viable options: inflatable belts and compression belts. The inflatable belt prototype consists of a stiff outer layer of clothing material and two horizontal rings of inflatable belts that wrap around the user's torso, as shown in **Figure 5.3** below.

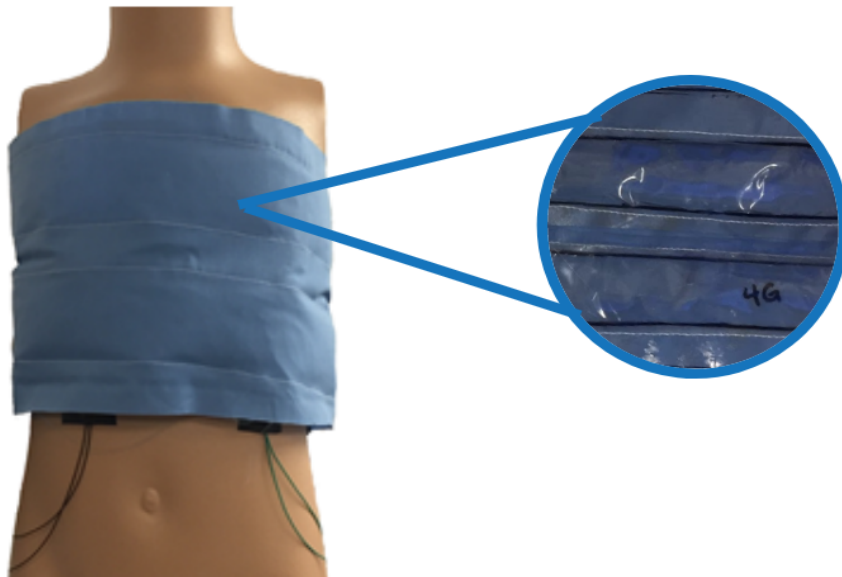


Figure 5.3: Image of Inflatable Prototype from Fall Semester.

5.1.2.1 Heat Transfer Model

The main mechanical challenges to address with the inflatable belt prototype were those of heat and moisture transfer in order to maximize comfort for the user. Because the inflatable belts would be made of airtight, impermeable material, a small air gap must separate the belts in order to let heat and moisture transfer from the user's body, through two clothing material layers, and out of the garment. To understand this process, the team analyzed heat transfer models using both a heat resistor network analysis calculated via MATLAB software (**Figure 5.4 (a)**) and a COMSOL FEA heat transfer analysis (**Figure 5.4 (b)**). Results of both models are plotted together (**Figure 5.4 (c)**), showing agreement between both analyses and a rough estimate of 20 W/m^2 transferring through the garment at 293K, or 20°C. The models' setups and results are shown in **Figure 5.4**.

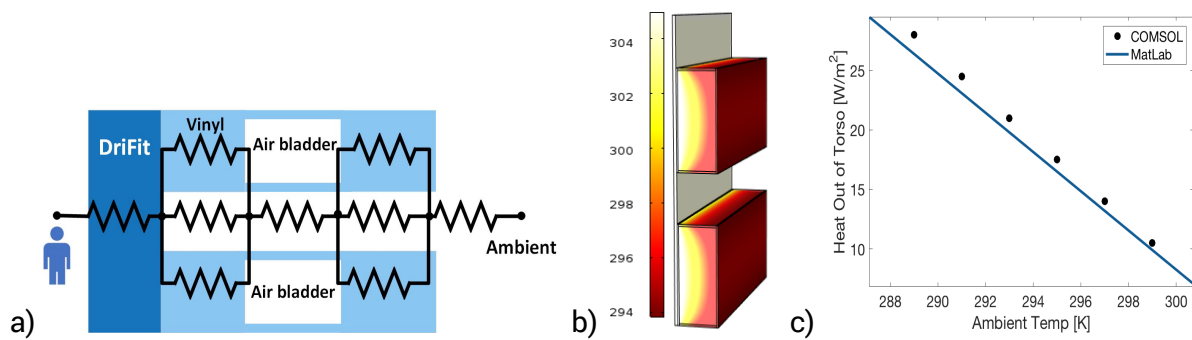


Figure 5.4: Heat Transfer Models

The heat resistor network shown in **Figure 5.4 (a)** was calculated using MATLAB software. Material thermal conductivity properties were taken from the COMSOL materials library, while air in the bladder is assumed to be dry air at 300K and the free convection standard yields a heat transfer coefficient between the HUGS outer material layer and ambient of $5 \text{ W/m}^2\text{-K}$. Thermal resistance for conduction is defined as,

$$R_i = \frac{t}{k'} \quad (1)$$

where R_i is the thermal resistance of layer "i" (e.g. Inner Layer, Outer Layer, and air section between) [$\text{K}\cdot\text{m}^2/\text{W}$], t is the material thickness [m], and k is the material's thermal conductivity [$\text{W}/\text{m}\cdot\text{K}$]. R_{total} , or the total thermal resistance of the prototype, is additive, so,

$$R_{total} = \sum_i R_i. \quad (2)$$

The total heat transferred from the user's body to ambient, q_{total} , is then,

$$q_{total} = \frac{\Delta T}{R_{total}}, \quad (3)$$

where ΔT is the difference between average torso temperature and the ambient temperature [K]. The full analysis is shown in the Appendix, Figure A7. The results of this heat resistor network calculation were verified with a finite element analysis model run in COMSOL (445_Inflatable_HeatTransfer1.mph), shown in **Figure 5.4 (b)**, using the same material parameters. It is important to note that, because the goal of these analyses was primarily for the team's understanding of the heat transfer theory through the HUGS materials, parameter values in these models were chosen only to the precision of order of magnitude. Agreement between these models, shown in **Figure 5.4c**, assures that a comfortable amount of heat (very

roughly $20 \text{ W/m}^2\text{-K}$) will transfer from the user to ambient in typical ambient temperatures of around 293K.

5.1.2.2 Design

The inflatable prototype consists of two rings of air-filled belts stitched onto a stiff outer material. This stiffness is necessary because the air bladders must inflate inwards rather than outwards for two reasons: (1) to maximize the efficiency of air inflation from the pumps applying deep pressure therapy effects felt by the user, and (2) to minimize the external profile of the system, allowing for the user to wear and use the device discreetly. At this stage in prototyping, the outer material stiffness need not be characterized, as it is more important to iterate through the manufacturing process of the airtight belts.

5.1.2.3 Manufacturing

The two main manufacturing challenges for the two-ring prototype are (1) achieving airtight seals and (2) integrating the inflatable belts with the outer material layer.

The team manufactured the inflatable belts by folding 4-gauge clear vinyl onto itself and heat-sealing it using a clothing iron, being sure to place a piece of parchment paper between the heat source and vinyl material during the process. This manufacturing decision was made after experimenting with a variety of tools including a typical soldering iron and heat gun. The typical soldering iron tip concentrated heat into too small of an area, causing holes to quickly burn through the vinyl material. On the other hand, the heat gun distributed heat over too great of an area, often causing the entire belt to seal on itself and making it nearly impossible to precisely control a straight-line seal. A clothing iron, however, produces even heat distribution with the ability to iron along a straight line for precise sealing. Because the belts are manufactured individually for this prototype, the large size of the iron's plate is irrelevant for this build. Further manufacturing decisions of the full-sized HUGS will be discussed later in this report.

Fitted to each of the belts is a 3-inch piece of flexible vinyl tubing that connects one of two air pumps to the belts. A hole is cut in the bladders on the inner garment side, the tubing is placed inside slightly, and hot glue is applied generously around the tubing to ensure an airtight seal.

The team used a sewing machine to stitch the belts to the outer material. This allowed for a strong, aesthetically appealing interface between the belts and the outer layer.

5.1.3 Compression Belt Prototype

Based on the down-selection discussed previously, we also moved forward with a compression belt prototype. The compression belt prototype consisted of two motors, two shafts, and fabric belts.

5.1.3.1 Material Analysis

We down-selected materials for the compression belt system based on mechanical properties. While heat transfer was a critical part of the inflatable belts prototype, it is far less important

here as there is only one layer of fabric and no air pockets to act as insulators. To compare various fabrics' mechanical properties, we utilized the MTS testing machine. We tested a 2-inch wide piece of five different fabrics: Nylon, Kevlar, Burlap, Blackboard, and Black Strap. **Figure 5.5** shows the stress vs. strain curves from the data gathered by the MTS machine. The gray area of the figure shows where an ideal fabric would fall. Anything to the left and above the gray area begins to act like a metal, taking on large stresses with minimal strain. While this would help us apply more pressure with fewer revolutions of the motor, materials in this area are too uncomfortable to wear on the body. Anything to the right and below the gray area experience too much strain at low stresses. These materials are not viable because they would be inefficient at applying pressure. For example, Burlap strains almost 10% before applying any significant pressure. This means the motor would be turning without applying much pressure at all. Thus, we down selected to three potential fabrics for the compression belt prototype Nylon, Blackboard, and Kevlar.

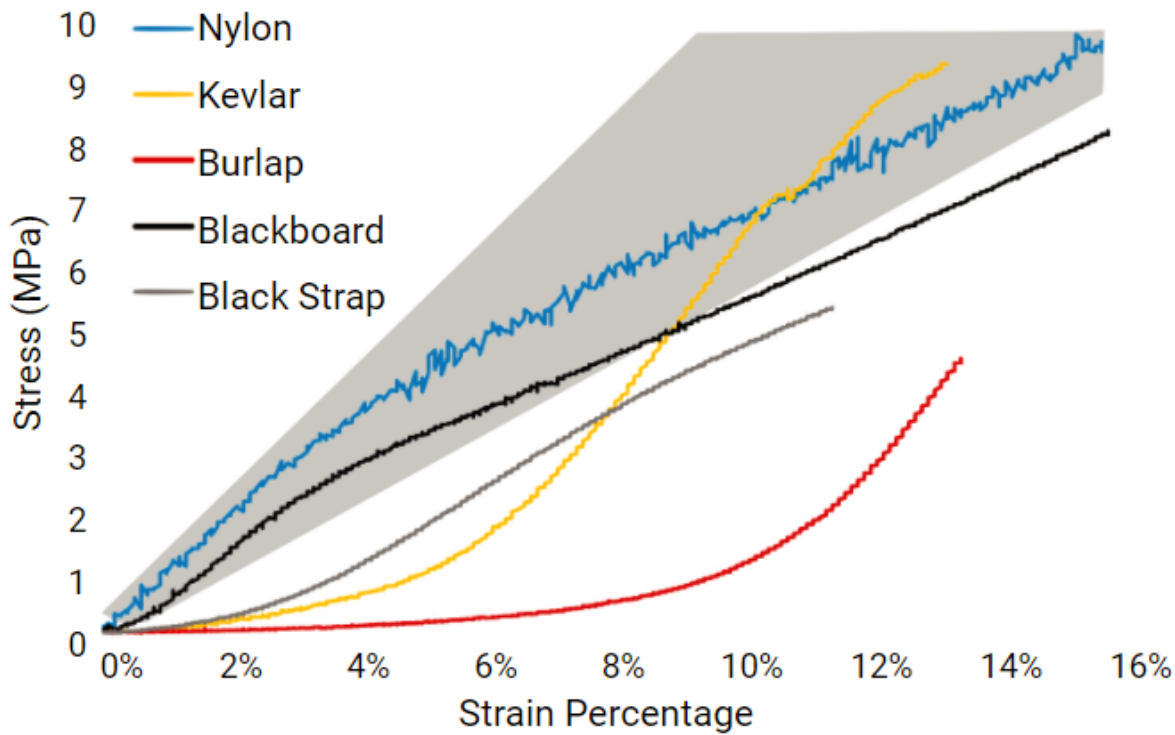


Figure 5.5: Graph of MTS Data for 5 Materials

5.1.3.2 Design

Due to the wearable nature of the device, we needed a motor system that was small and lightweight. Additionally, our ideal motor would be capable of motion in both directions and be able to hold its state for the duration of applied pressure. There are three main categories of motors which can be used for this situation: a DC motor, a stepper motor, and a servo motor. The standard DC motor can include both brushed and brushless varieties and would be a valid selection for this application due to its linear torque-speed relationship and manageability through the use of an encoder. A servo has more precise rotation tracking than a DC motor but has a limited range of rotation, often approximately 200 degrees in each direction. Since the

diameter of the shaft must be minimized for comfort, this realm makes a servo an unreasonable solution. The last option is a stepper, which is similar to a DC motor but optimized to hold a steady-state position due to the use of rotors in place of magnetic coils. Since the applied pressure state must be held constant for a prolonged period, the precision of a stepper is greater than that of a DC motor, and steppers are generally smaller and less expensive than DC motors. Thus, a stepper motor was the appropriate choice for the system. Due to the complication, mass, and discomfort of gear train systems, the stepper was selected such that it can direct-drive shafts.

5.1.3.3 Manufacturing

To build our compression belt prototype, we had to manufacture shafts to interface with both the motors and the fabric belts. We first attempted to 3D print our shafts on the TazBots, but due to the high aspect ratio of the shafts and warping on the print bed, the print failed. We then utilized the ProJet printer. While these shafts were successfully printed (**Figure 5.6 (a)**), the print took 55 hours. Finally, we machined usable shafts in about 5 hours (**Figure 5.6 (b)**).

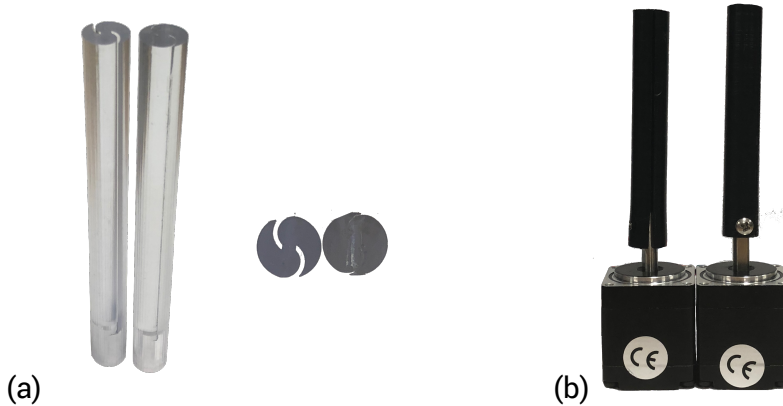


Figure 5.6: Images of ProJet Printed Shafts and Machined Shafts

Manufacturing played a role in down-selecting between the final three fabrics as well. The Nylon fabric, when cut into strips, would begin to fall apart when handled too much. Additionally, it became clear that the thicker Blackboard fabric had a significantly larger minimum radius than the Kevlar, which put a limit on how thin our shafts could be if we chose the Blackboard fabric. This led us to ultimately choose Kevlar as our compression belt material.

The final compression belt prototype consisted of two motors, two shafts, and two belts of Kevlar fabric. It is shown below in **Figure 5.7**.

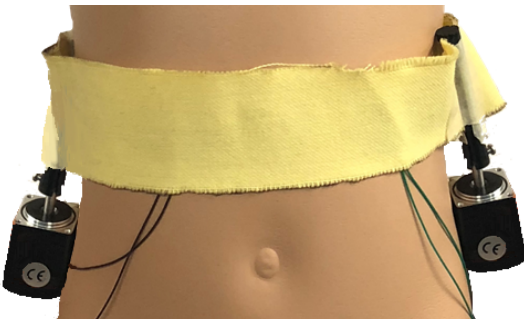


Figure 5.7: Compression Belt Prototype

5.1.4 Secondary Design Down Selection

Once the two aforementioned prototypes were constructed the team down selected between the two based on a number of selection criteria.

The first of these was weight. The expected total weight of the full-scale inflatable prototype was calculated to be 435 g based on a 2-inch belt weight of 159 g. This was 55 g less than that of the expected weight for the compression belt prototype of 490 g, based on a 2-inch belt weight of 242 g.

The second criterion was noise at 1 meter. The inflatable prototype had a noise level of 42 decibels, while the compression belt prototype had a noise level of 52 decibels.

The final criterion was uniformity of pressure distribution. **Figure 5.8** shows the standardized (unitless) pressure distribution outputs of one ring of six pressure sensors on the test setup. Observationally, the inflatable belt pressure distribution (**Figure 5.8 (b)**) appeared to be more uniform. Additionally, when using dimensioned data, the standard deviation of the compression belt pressure distribution (**Figure 5.8 (a)**) was 5.27 kPa, while it was 3.56 kPa for the inflatable belt pressure distribution.

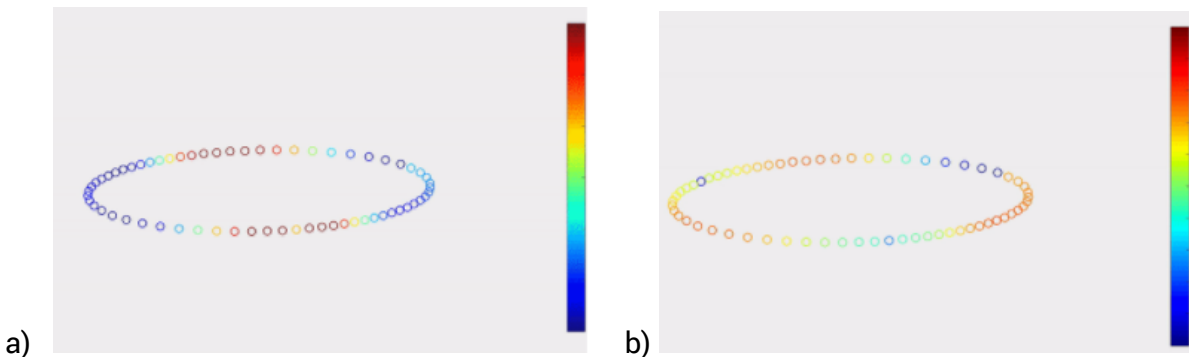


Figure 5.8: Pressure Distributions for (a) Compression Belt, (b) Inflatable Belt Prototypes

These results are also supported by a mathematical analysis performed with the help of Dr. Michael Carchidi on the force applied by the compression belt mechanism. The analysis looked

at the distribution of pressure along the perimeter of the torso when there is tension applied from two points at the ends of the major axis, as shown in **Figure 5.9**.

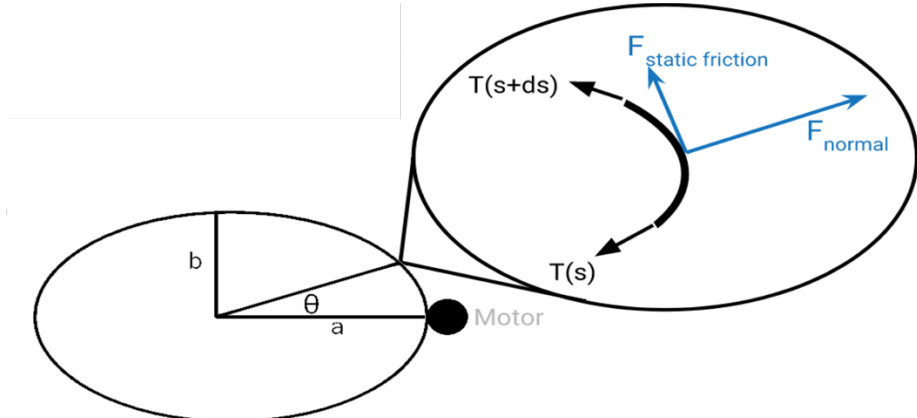


Figure 5.9: Diagram of Mathematical Analysis on Applied Force on Ellipse

This analysis concluded that the tension applied on the body would be governed by the following Bessel function, where a and b are the lengths of the major and minor axes, as shown in **Figure 5.9** and s is the tension in the material:

$$T(\theta) = T_0 e^{-\mu s \tan^{-1} \left(\frac{a \tan(\theta)}{b} \right)} \quad (4)$$

According to this equation, it is impossible to achieve a uniform pressure distribution when the force is applied via a motor affixed to one point. This assured us that the inflatable prototype would apply a more uniform pressure distribution than the compression belt prototype.

Due to the inflatable belt prototype outperforming the compression belt prototype on these three metrics, the team continued with the inflatable belt system.

5.2 Mechanical

The following section details the mechanical design process for HUGS, including the materials used, the geometry of the system, and the manufacturing process.

5.2.1 Material Selection

The materials in HUGS were selected on two metrics: absorptivity and comfort. The selection processes are detailed below.

5.2.1.1 Material Selection for Absorptivity

We performed moisture wicking tests on six fabrics shown in **Figure 5.10**. The six fabrics are, from left to right, Cotton, 90% Polyester 10% Spandex, Polyester, Quilting fabric, Nylon, and Polyester Blend. We exposed each fabric to the same volume of water (~2ml) for 10 seconds, then recorded the drying time of each to determine its moisture wicking capabilities.

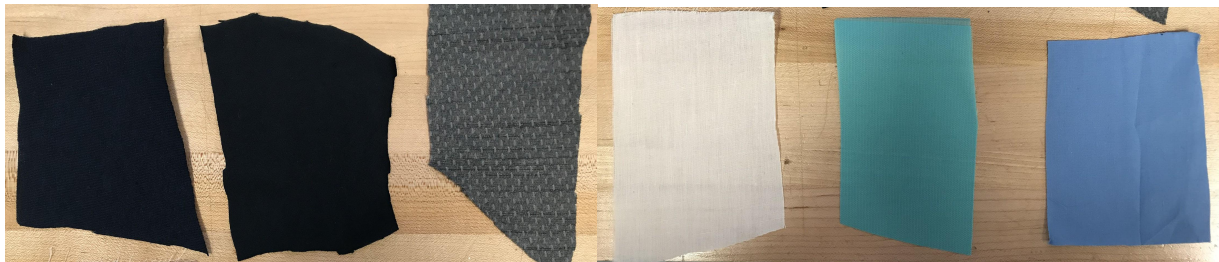


Figure 5.10: Fabrics Used for Moisture Test

Table 5.7 shows the drying time results and observations from the test. As expected, cotton performed poorly and was still very wet even 35 minutes after exposure to the water. The best performers were Quilting Fabric, with a dry time of 11 minutes, and Polyester Blend with a dry time of 10 minutes. We used this data to down-select our fabrics to three materials, Quilting Fabric, Polyester Blend, and Polyester. The decision to keep Polyester over Nylon was because the Nylon never really soaked up the water, while the Polyester was the only fabric to soak up all the water. This comparison is shown in **Figure 5.11**. Because of this, we determined that the Polyester would be a superior moisture wicking material than the Nylon.

Table 5.7: Moisture Testing Results

Material	Evaporation time	Observations (10s wetting)	Observations (drying)
Cotton (dark blue)	35+ min	Soaked up a lot of water	Did not dry
90% Polyester/10% Spandex (dark blue)	0 min	Soaked up no water	n/a
Polyester (gray)	27 min	Soaked up quite a bit of water	Still damp when visibly dry
Quilting Fabric (white)	11 min	Soaked up small amount of water	Dried quickly, still slightly damp once visibly dry
Nylon (aqua)	18 min	Most water was on surface, not soaked up	Slightly damp when visibly dry
Polyester Blend (blue)	10 min	Soaked up small amount	Dried very quickly, no dampness

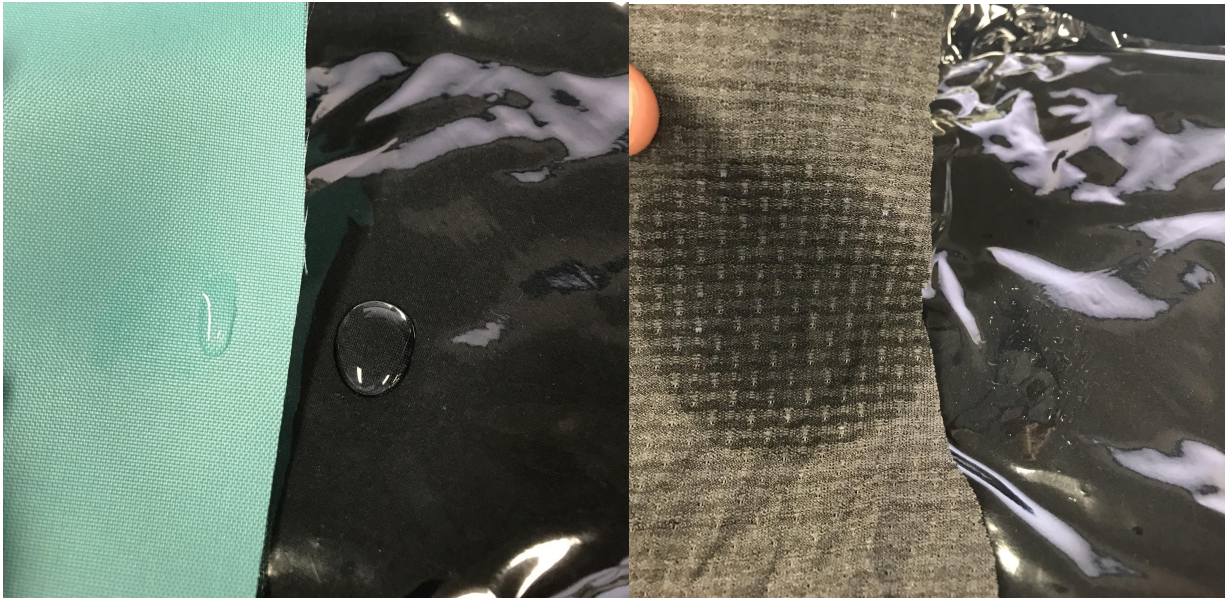


Figure 5.10: Comparison Between Nylon (left) and Polyester (right) Water Absorptivity

5.2.1.2 Material Selection for Comfort

After down selecting from six fabrics to three, we conducted a running test to determine which combination of fabric would be the most comfortable for the wearing, as well as which would wick away the most sweat. A team member ran 4 different times—resting between each test. Each time the team member ran at 12 mph for 0.25 miles, then at 6 mph for 0.15 miles, then at 12 mph for another 0.10 miles to build up a sweat. The team member then rested for 2 minutes before the material was weighed for moisture. The material was then allowed to dry until the mass of the material again matched the starting mass. After running, the team member was asked to evaluate three metrics—skin contact comfort, movability, and how hot the material felt—on a scale from 1 to 5. All this data was collected and compiled in **Table 5.8** below. For simplicity, Polyester blend is denoted as “Blue”, Quilting fabric as “White” and Polyester as “Gray”.

Table 5.8: Material Performance in Running and Comfort Tests

Test	Outer	Inner	Start	Finish	Dry Time	Contact Comfort	Movability	How Hot	Cumulative Comfort
1	Baseline	Baseline	146	149	5	5.0	5.0	1.0	93.3
2	Blue	White	128	131	10	3.5	4.0	4.5	59.3
3	Blue	Gray	144	146	8	4.5	4.0	3.5	72.3
4	White	Gray	134	136	10	4.5	4.0	2.5	74.7

A cumulative comfort score (max of 100) was calculated by weighing 5 different categories equally. These categories were: (1) water mass added during run, (2) grams dried as a function of time, (3) contact comfort, (4) movability, and (5) how hot the material felt. Scoring the best (93.3) was the baseline test of the athletic t-shirt with no inflatables, as expected. However, of the three material combinations tested for HUGS, the Quilting fabric outer with the Polyester inner scored the best, with a score of 74.7.

From the testing, the team inferred that this combination scored the highest because the Quilting fabric was more porous than the Polyester. This gave the team the idea that using a mesh as the outer material would yield an even higher comfortability score, without any sacrifice in functionality. We then performed the same test on a combination of Mesh outer, bladders, and Polyester inner to determine the final material pair for HUGS. As shown in **Figure 5.11**, the mesh and polyester combination were the highest scoring combination.

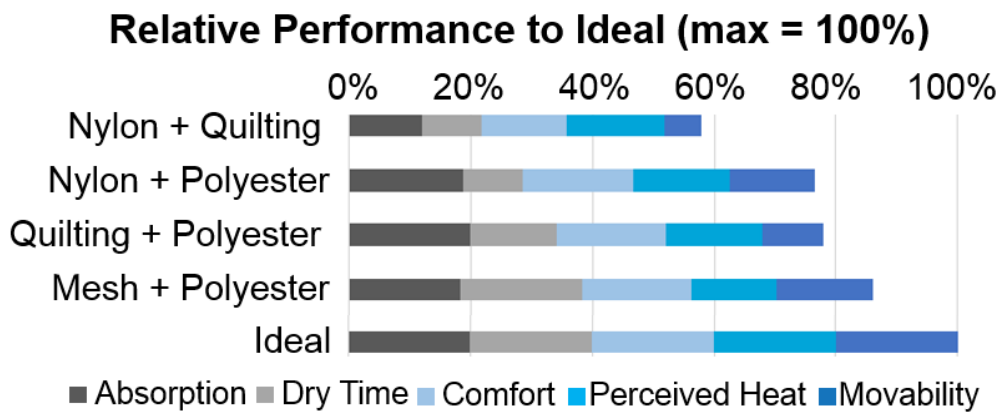


Figure 5.11: Running and Comfort Test Results

5.2.1.3 Overall Material Selection

Based on the moisture absorption test and the comfort test, the final materials selected for the HUGS device were Polyester for the inner layer and Mesh for the outer layer. The Polyester did well in the moisture absorption tests, and performed better than the other possible inner material, Quilting fabric, in the comfort tests. Mesh was never tested in the absorption tests because it is not necessary as it is the outer fabric. The most important role that the outer fabric plays is keeping the bladders from expanding outward and facilitating moisture/heat transfer away from the body. With small holes uniformly distributed across the fabric, the mesh allows for heat transfer from the body, demonstrated by its high perceived heat score in the previous figure. Stiffness of the bladders and materials will be covered in the following section.

5.2.2 Bladder Geometry

The geometry of the inflatable bladder pockets was determined through quantitative analyses on stiffness, heat and mass transfer from the body to the ambient, perceived heat, and perceived perception of uniformity.

5.2.2.1 Stiffness Analysis for Bladder Geometry

As stated before, the air bladders need to inflate inwards versus outward so that pressure application is as efficient as possible but also to ensure that the device is as discreet as possible. A simple high-level analysis performed with Dr. Bruce Kothmann showed that the system of the body and bladders can be looked at like a series of springs (**Figure 5.12**).

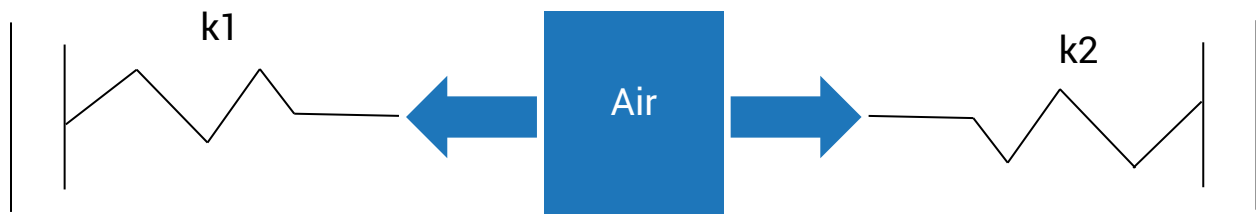


Figure 5.12: Springs in Series with Force from Air Bladders

The body and the bladder outer walls can be treated as springs and the air in the bladders is just a force pressing against the two of them. As the bladders fill up, it applies a force against the body and the back wall of the bladders. The formula for equivalent spring constant for springs in series is

$$k_{eff} = \frac{k_1 k_2}{k_1 + k_2} \quad (5)$$

If the body is significantly stiffer than the bladders, then the internal pressure will cause the system to expand out. This means we want to optimize stiffness of the bladders via our material selection and geometry. The differences in measured stiffnesses for the three gauges of vinyl we tested were negligible, so geometry became more important. For this reason, we made the bladders a lopsided semicircle. The top of the bladder is an arc with a length of 1.6 in and the bottom is flat with a length of 1 in shown in **Figure 5.13**. This makes it so that the full expansion of the back side of the bladder occurs before the full expansion of the front effectively making the back stiffer.

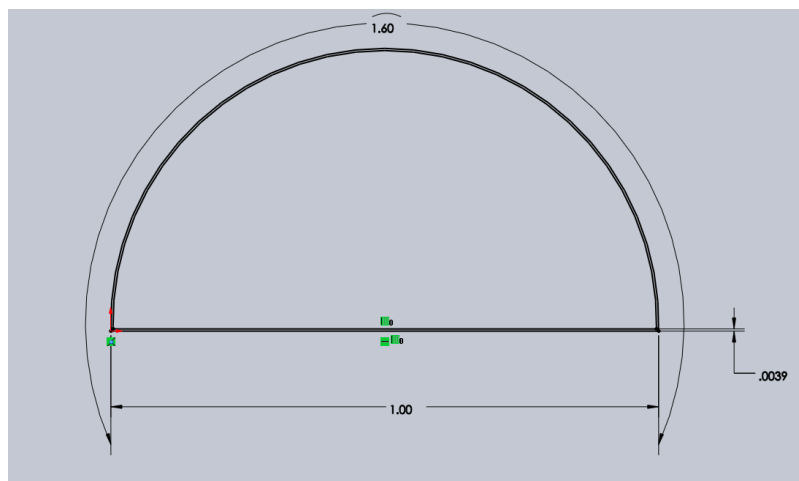


Figure 5.13: Cross Section of Bladder Geometry

5.2.2.2 Effect of Bladder Size on Heat and Mass Transfer

The user will be wearing HUGS under their regular clothes so we want to make sure that HUGS doesn't overheat the user. We performed a heat transfer analysis to help determine the optimal spacing between each bladder to maximize heat transfer without compromising pressure distribution. After speaking with our advisor, Dr. Lukes, it was clear that we wanted natural convection to occur between the bladders since the bladders are insulators and air circulation between the bladders would help with cooling the user.

Based off this information, we calculated the Rayleigh number for HUGS, a dimensionless parameter that determines whether free convection occurs in a fluid. **Figure 5.14** shows a graph of our calculated Rayleigh number as a function of gap spacing. The blue line is our Rayleigh number, the orange line is the threshold for natural convection, and the grey line is a 1.5 safety factor for the threshold. The graph tells us as long as we have a gap of about 1.5 cm or more then natural convection should occur, helping with heat transfer.

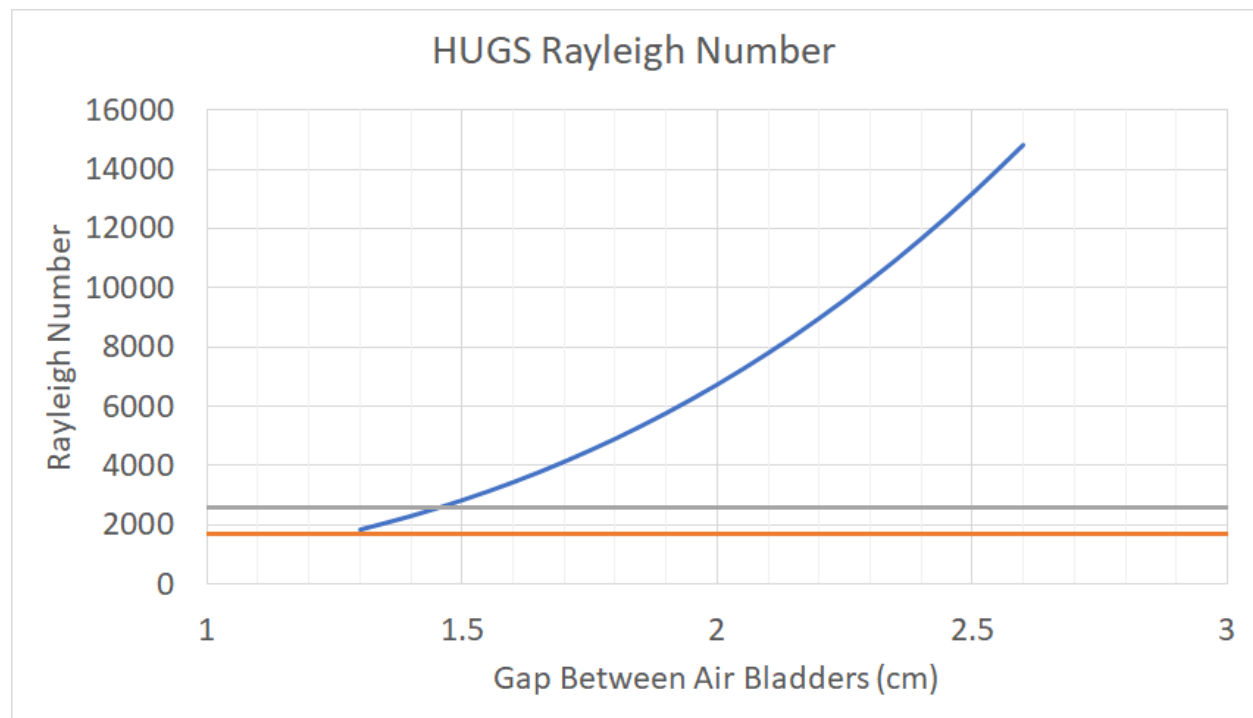


Figure 5.14: Graph of HUGS Rayleigh Number as Function of Bladder Spacing

5.2.2.3 Effect of Bladder Size on Perceived Heat

Using the calculated Rayleigh numbers, we utilized the correlation for internal free convection in a vertical rectangular cavity to find the average Nusselt number of each air gap spacing. This was the closest correlation to our bladder shape that we could find.

$$\overline{Nu_L} = 0.18 \left(\frac{\Pr}{\Pr + 0.2} Ra_L \right)^{0.29} \quad (6)$$

Using the calculated Nusselt Number, we found “h”, the heat transfer coefficient. These values were used in a simple heat resistor network of one bladder and one air gap in parallel to calculate the body temperature deviation from usual torso temperature. **Figure 5.15** below shows the torso temperature deviation as a function of air bladder gap spacing. There are too many factors dependent on individual people (e.g. heat flux from body, sweat rate, and external environment) to definitively determine actual torso temperature while wearing HUGS. However, this model does show us the expected decrease in temperature as air gap spacing increases, therefore validating our decision to make the air gap as large as possible while maintaining uniform pressure. The MATLAB code written for this simulation is in the Appendix, Figure A6.

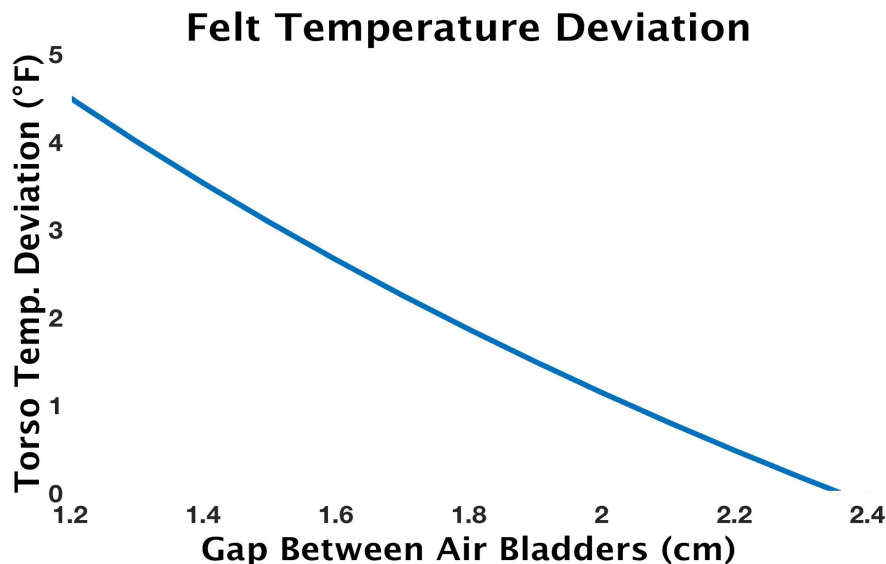


Figure 5.15: Temperature deviation as a function of air bladder spacing

5.2.2.4 Effect of Bladder Size on Perceived Uniformity

We performed a touch test to create a distribution of the distances at which people perceive one point of contact versus two. This, along with the heat transfer analysis discussed above, helped us choose an appropriate bladder spacing for our prototype. Previous research has shown that perception of two contact points varies based on both location on the body and direction (i.e. horizontal, vertical) [31]. While there is extensive research into human perception of touch, no currently published studies had data for our specific needs [32] [33]. Thus, we created a touch test in order to determine the maximum distance between two points at which a person still perceives one point of contact on the torso.

We used calipers, with small safety shields to prevent injury from the sharp points, as our touching device to ensure accurate distances. For each test subject ($n=110$) we took 8 measurements on the middle back area at a gap spacing of 5, 10, 15, 20, 25, 30, 35, and 40mm. Each participant was asked to remain still and, after each touch, express whether they perceived

one or two points of contact. In order to avoid any bias introduced by the anchoring effect, we used a random number generator to randomize the order of the distances for each participant. We also recorded each participant's height to determine if the smaller size of our target audience could have an effect on touch perception. Each subject was tested through only one layer of clothing in order to remove a potentially confounding variable.

The data from the touch tests is shown below in **Figure 5.16**.

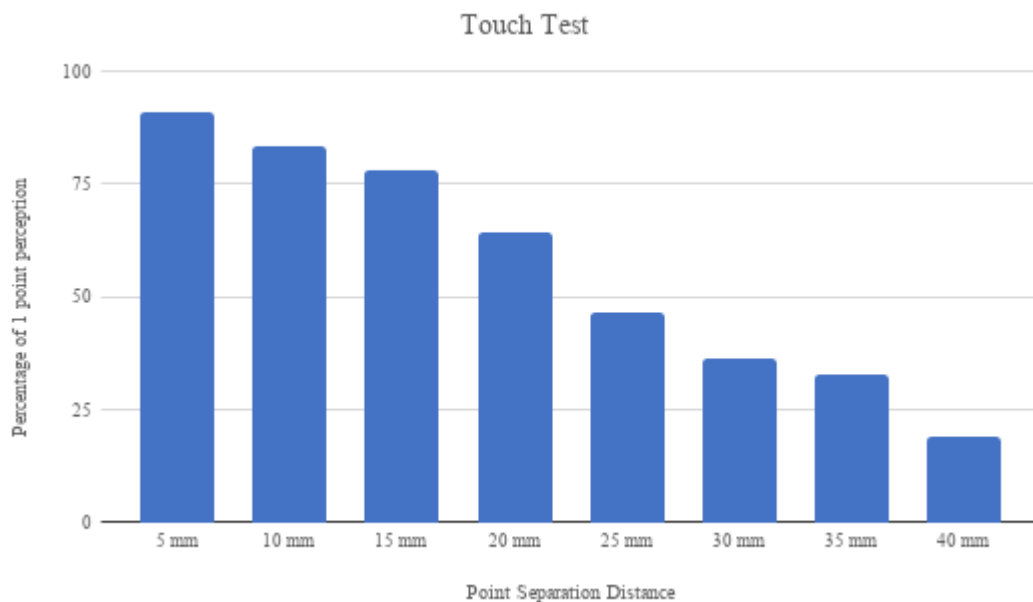


Figure 5.16: Touch test results

5.2.2.5 Bladder Geometry Selection

Figure 5.17 is a graph with the touch test we performed along with our Rayleigh number calculations. Both are a function of bladder spacing. The yellow line is the data for the touch test, the blue line is the Rayleigh number calculation, the red line is the natural convection threshold, and the black line is our 1.5 safety factor. From this graph we were able to optimize our bladder spacing at 1.6 cm. This allows us to have a Rayleigh number above our 1.5 safety factor, about 70% of people perceiving 1 point of contact (pressure uniformity), and a perceived temperature deviation of about 2.5 degrees Fahrenheit.

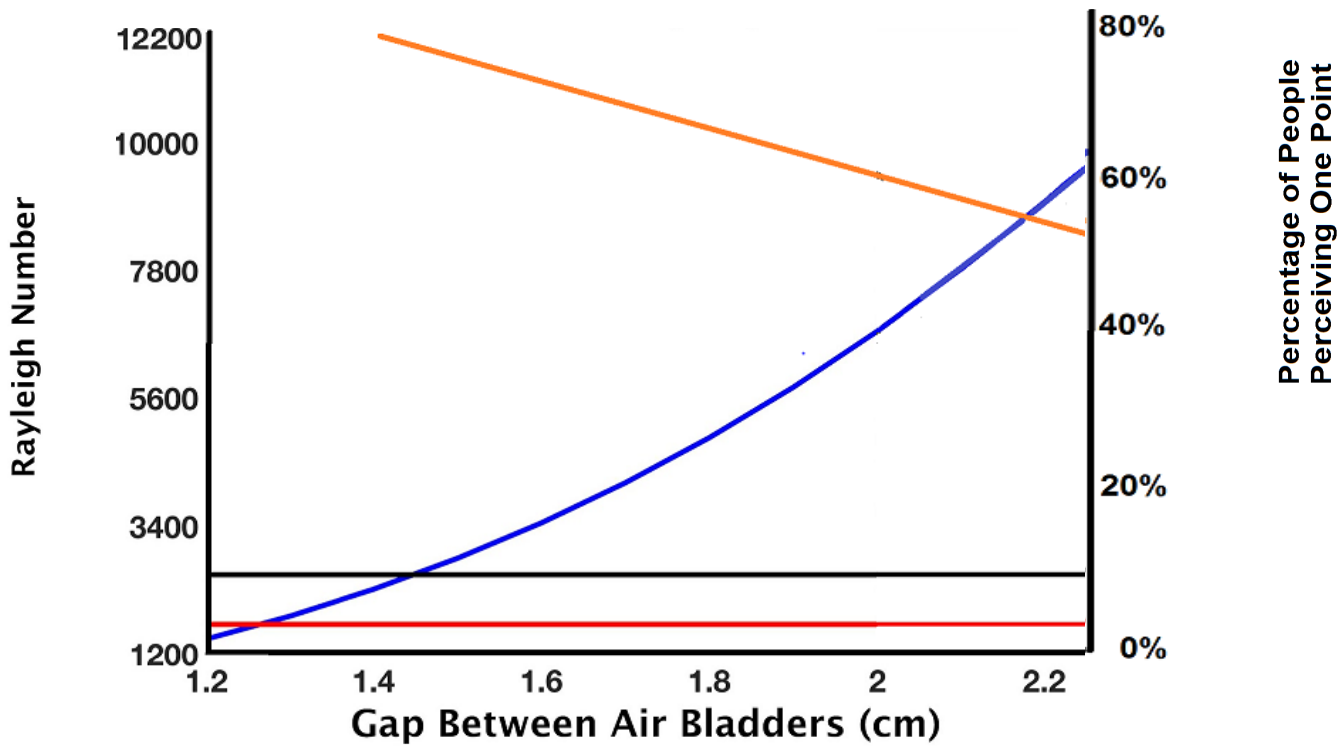


Figure 5.17: Rayleigh Number and Touch Test Results as Function of Gap Spacing

With the spacing set at 1.6 cm (about 0.63 in) and the bladders having a 1 in flat side length we are able to manufacture the entire vest with 5 bladders that go around the entire torso and 2 additional bladders that apply pressure to the upper back (around the shoulder area).

5.2.3 Manufacturing

The HUGS garment was manufactured to contain three layers: inflatable bladders which lay between an inner material in contact with the child's skin and an outer fabric on the extremity of the garment.

5.2.3.1 Bladders

The central bladders are constructed from one large sheet of 4-gage vinyl plastic. The sheet is folded over on itself and ironed together in order to create a fully connected system of bladder rings that wrap around the user's torso. **Figure 5.18** below shows the starting pattern that is traced onto a 71.1cm by 49cm flat sheet. The central bladders consist of 7 horizontal rings with four vertical channels. The vertical channels allow airflow to all rings while only requiring two pump entry points. As discussed in the Bladder Geometry section, the gap spacing between rings is 1.6cm. When inflated, each ring is a semi-circle. Thus, the outer side of the ring is 2.5cm, while the inner side, which inflates in towards the user, is 4cm.

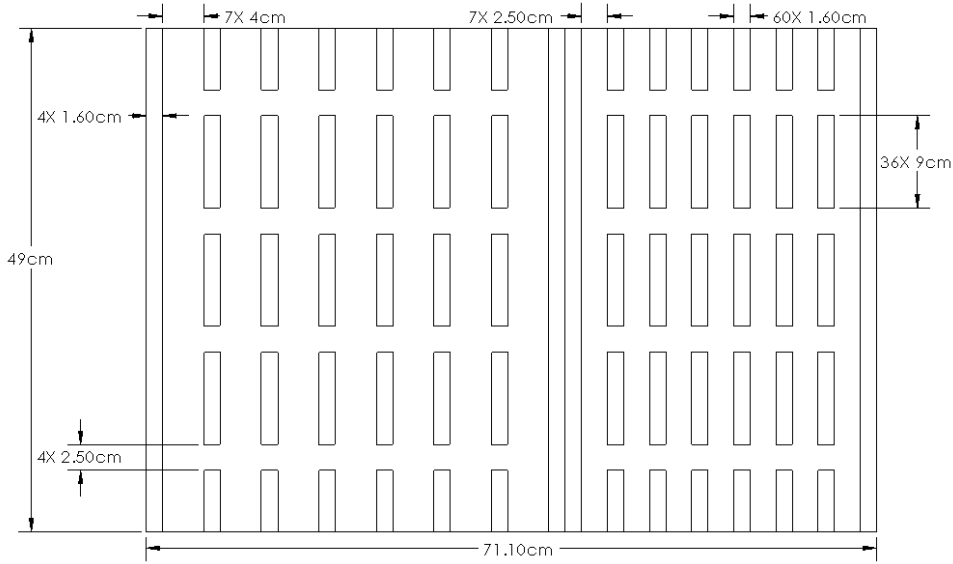


Figure 5.18: Original pattern traced for HUGS' central bladders

Next, the sheet is folded onto itself and the horizontal rings are positioned such that the iron can easily seal all of the gap spacing. This process is shown in **Figure 5.19**.

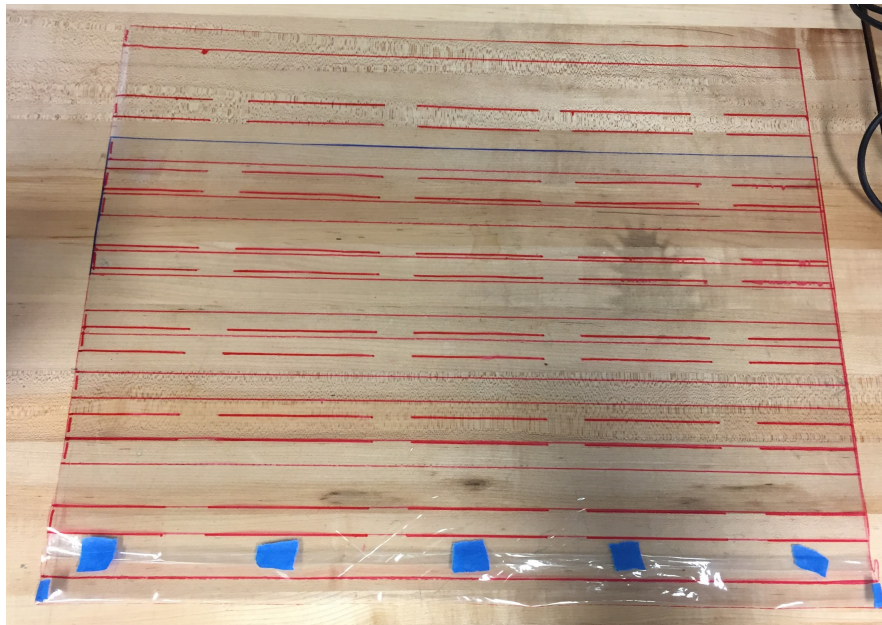


Figure 5.19 Step 1 of Central Bladder System Manufacturing Process

Next, the gap spacing is sealed using a Portasol Butane Soldering Iron and its paint scraping tip, operating at approximately 300 °C. While the clothing iron discussed in the Inflatable Belts Prototype section created a strong seal, it was too large to be able to seal thin strips. Thus, the butane iron's tip was custom machined to a thickness of 1.6cm, allowing an accurate and precise gap spacing seal. This process and the resultant seal are shown in **Figure 5.20 (a)** and

Figure 5.20 (b). To avoid melting the vinyl completely, parchment paper surrounds the vinyl sheet during the ironing process.

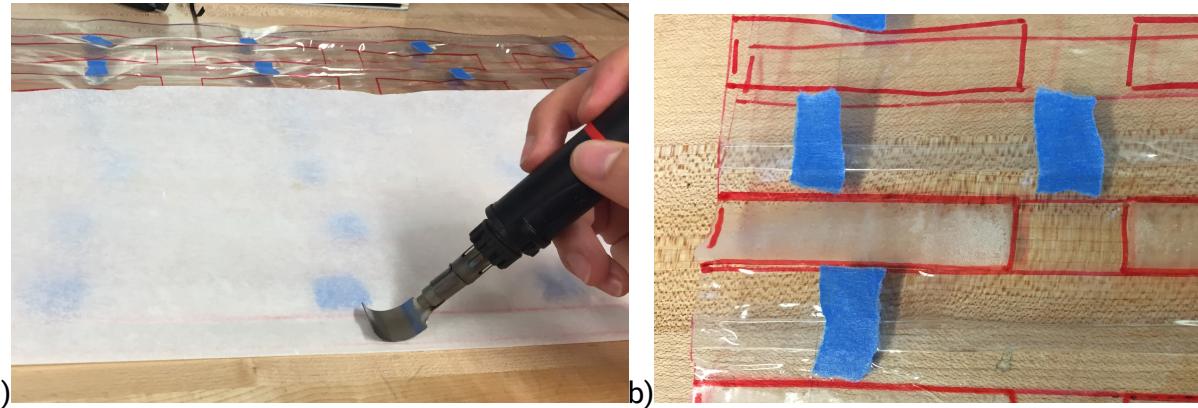


Figure 5.20: Step 2 of Central Bladder System Manufacturing Process

The ends of the top two rings are cut out and sealed to allow space for the user's arms, as shown in **Figure 5.21 (a)**. The ends of the bladder rings are also sealed such that no air can get in or out of the central bladder system. Next, the air gaps are cut out using an X-ACTO knife. 4mm are left to seal the bladder rings on each side, while the remaining rectangle is cut out as shown in **Figure 5.21 (b)**.

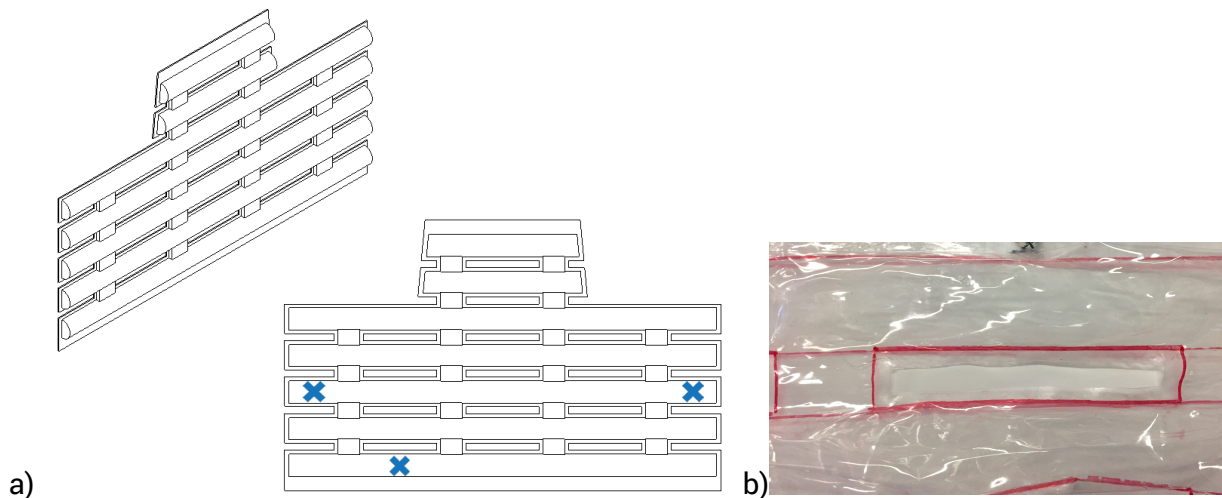


Figure 5.21: a) Final Air Bladder System Design b) Close up of the air gap cutouts.

Lastly, tubing is fitted to the bladder in three spots: one point of entry for each of the two pumps, and one point of exit for the solenoid release mechanism, as shown by the blue "X" markers in **Figure 5.21 (a)**. A hole is cut in the bladders on the inner garment side, the tubing is placed inside slightly, and hot glue is applied generously around the tubing to ensure an airtight seal. An example of this connection is shown in **Figure 5.22**.



Figure 5.22 Tubing to Bladder Sealed using Hot Glue.

5.2.3.2 Inner Material

As discussed in the Material Selection Section, the inner material is made of 100% polyester. A youth x-small 100% polyester athletic shirt is cut and tailored to fit the user, which in this case is the pressure testing mannequin. The inner layer is shown in **Figure 5.23** below. Because HUGS is an undergarment to be worn by children with ASD every day, it must be machine washable. As such, the machine-washable inner material is fitted with zippers on either end and buttons across the top and bottom which all integrate with zippers and buttons on the outer material. These connections allow it to be completely removed from the outer layer and central bladders. Both the zippers and buttons are sewn into the inner material.



Figure 5.23: HUGS Inner Layer with Zippers

5.2.3.3 Outer Material

As discussed in the Material Section, the outer material is made of nylon mesh. Similar to the inner material, an athletic pinnie is cut down and tailored to fit the user. Zippers and buttons are sewn in to this layer in order to integrate the inner material with the outer material. Additionally, a zipper is sewn onto the front, allowing the garment to zip up the front of the user's torso like a typical vest.

5.3 Hardware, Software

The HUGS system uses biometric and environmental sensors to take inputs from the environment and operates on those inputs onboard the device. The following section details the sensor selection process, then the system architecture and communication decisions, as well the choice of controller for the device. It then covers the electrical components, calibration, the onboard software, and the accompanying mobile application.

5.3.1 Sensor Selection

The team needed to determine which sensors would be used in the final system prototype for establishing thresholds on which to activate. Initially, the team pitched using solely two biometric sensors, a heart rate sensor and a galvanic skin response sensor, to measure the current state of the user. This was based on preliminary conversations with occupational therapists the team had early on in the design process when establishing the utility of the system.

Looking for advice on the implementation of sensors, the team contacted and met with Dr. Daniel Bogen, a retired Bioengineering professor at the University of Pennsylvania. Dr. Bogen's research focused primarily on pediatric therapeutic medicine and was thus trusted as an expert in this field. In talking with Dr. Bogen, the team learned that biometric sensors such breathing rate and skin response are difficult to measure and are often inaccurate, and thus have limited utility in a product such as this. Dr. Bogen did advise however that while still not easy to measure, a heart rate sensor would be very useful in the device. He also advised that external sensors, such as temperature, noise, light, and acceleration, can serve as good indicators for what triggers changes in a person's physical and emotional state and thus would be useful in the device.

As a result of the conversation with Dr. Bogen, the HUGS device utilized heart rate, temperature, noise, light, and acceleration sensors.

5.3.2 System Architecture

The HUGS system architecture consists of two primary components: an onboard circuit with closed-loop feedback control that reads in sensor inputs and determines pump inflation status, and an external mobile application that sets configurations for the onboard electronics. A block-diagram of this circuit is shown in **Figure 5.24**.

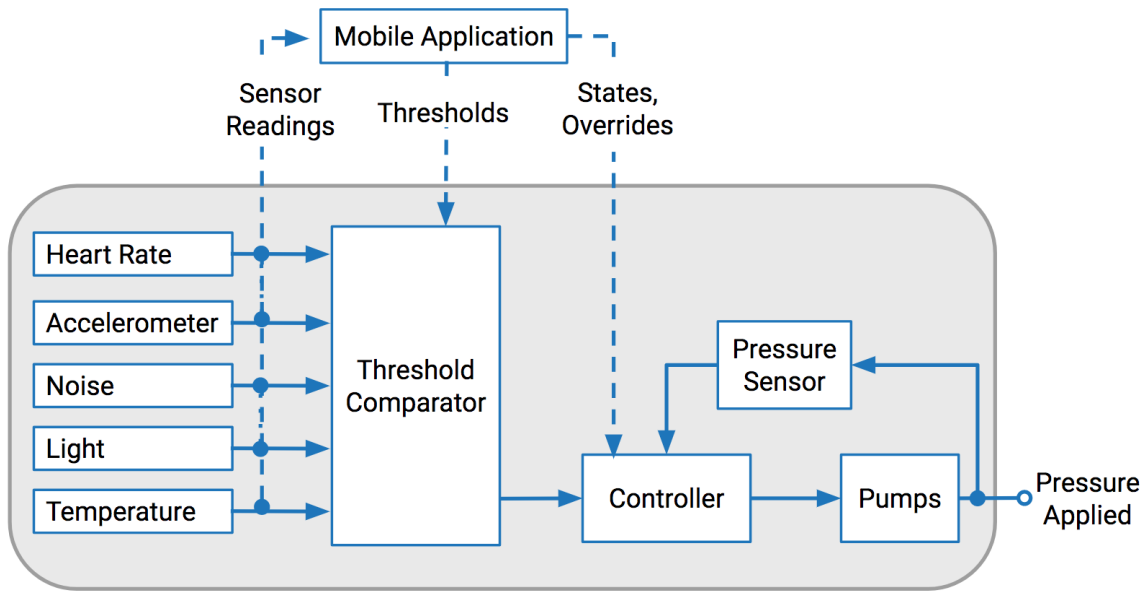


Figure 5.24 Block-Diagram of HUGS System Architecture

The gray region of **Figure 5.24** shows the onboard component of the HUGS electrical system. This component acts independently of the mobile application; once it receives the preliminary configuration data, the application need not be on or nearby for the system to operate. The onboard system takes inputs from five sensors: a heart rate sensor, a 3-axis accelerometer, a noise sensor, a light sensor, and a temperature sensor. These inputs are passed into a threshold comparator, which uses the values received from the mobile application in the configuration step and compares them to produce a binary output as to whether the bladders should be inflated. This goes into a controller. The controller takes feedback from an internal pressure sensor and combines it with a desired pressure level set by the mobile application to determine whether the pumps or solenoid should be activated to achieve the desired pressure level. The pumps increase inflation of the garment and the solenoid releases the stored air, thus reducing the pressure.

The dashed lines in the diagram in **Figure 5.24** show that the mobile application functions independently. The application receives information on the current status of each of the onboard sensors and transmits back information on thresholds and system states. The system has two primary modes: Manual, in which the device must be activated or deactivated using the application, and Proactive, in which the device uses the thresholds to determine the inflation status. The application also allows for the user to configure the desired pressure level using a slider on the application, as well as set which thresholds should be activated and at what levels they will trigger a response. This communication occurs via Bluetooth, and the HUGS device can communicate with the mobile application within a range of approximately 10 meters.

5.3.3 Communication and Data Storage

There are two implementation techniques for connecting a wearable to an external device. The first solution is to store the data on the device and communicate with the external device when within a reasonable range via Bluetooth or Wi-Fi connection. The second solution is to choose a microcontroller with an LTE-enabled chip that lets it store its data in a database in an external server. The data could then be accessed remotely from any location through a web interface. The second solution is more robust, as the first one requires the external device to be nearby to make changes. However, the latter is significantly more expensive, as it requires a data plan for the microcontroller with a recurring subscription as well as server space from an external platform, and also provides problem with data encryption since it would be publicly accessible. Therefore, HUGS is designed to communicate directly with the mobile application without the use of an external service.

The HUGS device uses Bluetooth Low Energy (BLE) to transmit data between the garment and the external application. Wi-Fi is a more robust system than Bluetooth for most forms of data transfer - it allows for transmission of larger files, 802.11ac and 802.11n can run orders of magnitude faster than even advanced Bluetooth protocols, and can transmit signals over much larger ranges. However, small processors with Wi-Fi capability are rare and expensive compared to their BLE counterparts, as BLE is the standard for most Internet of Things devices. Furthermore, the HUGS platform does not have large file in transmission, any weight/size constrained microcontroller would operate slower than the transmission rate of Wi-Fi, and BLE is easier to implement, it was decided to use BLE for the purposes of the HUGS application.

5.3.4 Microcontroller and Battery Selection

The HUGS garment operates on an [Adafruit Feather](#) 32u4 Bluefruit LE microcontroller. The device was selected for its small size, light weight, integrated support for a 3.7 V Lithium Ion Battery, BLE capabilities, and ten analog input pins. There were two battery sizes under consideration for HUGS: 3.7 V and 6.0 V. It is preferable to use a 3.7 V battery since the device is less hazardous as a wearable at a lower voltage. To determine the number of milli-amp hours required for the battery, we first needed to define the current use of the device. Measuring the current draw of each subsystem, we were able to set upper bounds, shown in **Table 5.9**.

Table 5.9: Current Draw of HUGS Components

Item	Current (mA)
Microcontroller (including BLE)	15 mA
Heart Rate Sensor	10 mA
Accelerometer	10 mA
Noise Sensor	2 mA
Light Sensor	2 mA
Temperature Sensor	2 mA
Internal Pressure Sensor	5 mA
Pump	250 mA (x2)
Solenoid	400 mA

Since all components except the pump and the solenoid are operating continuously, there is a continuous 46 mA of current draw. Thus, running continuously for a 10-hour period requires 460 mAh. The pumps are used continuously in inflation and are occasionally while in the inflated state to maintain a pressure value. We can therefore approximate that the pumps will be active no more than 2 hours of the 10-hour period. This adds a maximum current draw of 1000 mAh. The solenoid is used infrequently to deflate the device and will be active for no more than 1 hour of standard use, adding a maximum current draw of 400 mAh. Since this usage sums to 1860 mAh, HUGS runs on a 2000 mAh battery.

The Feather has 20 ports, 10 of which have analog capabilities. Furthermore, these pins are grouped into four packages, with current limits on each package. Since HUGS requires 8 analog inputs and 3 digital outputs, and since only the digital outputs run via current-controlled MOSFET circuitry, the pins had to be carefully selected in order for the device to run. The pins, which are referenced in the Electrical and Embedded software below follow the pinout below in **Table 5.10**. The formal information on the microcontroller can be found [here](#).

Table 5.10: Microcontroller Pin Delegation

Pin	Functionality	Use on HUGS
A0	Analog, Digital, Serial	Accelerometer X (Analog in)
A1	Analog, Digital, Serial	Accelerometer Y (Analog in)
A2	Analog, Digital, Serial	Accelerometer Z (Analog in)
A3	Analog, Digital, Serial	Noise Sensor (Analog in)
A4	Analog, Digital	Heart Rate Sensor (Analog in)
A5	Analog, Digital	Light Sensor (Analog in)
13	Digital	Pump Toggle (Digital out)
12	Analog (A11), Digital	Temperature Sensor (Analog in)
10	Analog (A10), Digital	Solenoid Toggle (Digital out)
6	Analog (A7), Digital	Internal Pressure Sensor (Analog in)
5	Digital	Pump Toggle (Digital out)

5.3.5 Electrical System

The layout of the full electrical system became fully constrained in the second semester of the course after meeting with Dr. Bogen. The components of the electrical design were a product of the environmental and biometric data to be collected and the physical responsiveness of the vest that was necessary to meet target goals.

Focusing first on the physical responsiveness of the system, the vest was equipped with two motors and a solenoid pressure release valve. Regardless of the inputs triggering the valve and the pumps, the operation of these actuators was vital to ensuring the vest met the physical responsiveness criteria set in the Binding Project Proposal - the pump had to fill the vest to a steady pressure within 20 seconds and the solenoid had to release air at a rate that would allow for steady state pressure to be released within 20 seconds to meet our goal.

The circuitry for the pump uses a low-power 2N7000 MOSFET to carry the current from the vest's LiPo battery to the pump when triggered from the controller's digital signal as shown in **Figure 5.25**. The 100Ω resistor was responsible for limiting current draw from the microcontroller while the $1M\Omega$ resistor was responsible for pulling the gate pin down to ground. The pump drew approximately 300-400mA.

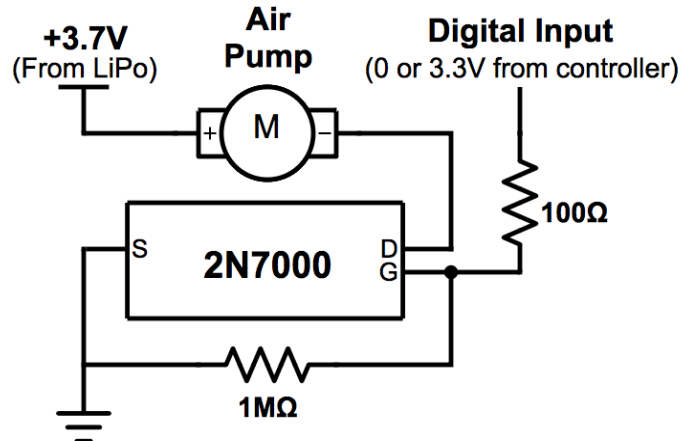


Figure 5.25: Air Pump Motor Driver Circuit

The circuitry for the solenoid used a high-power IRF630 MOSFET responsible to carry current from the vest's LiPo battery to the solenoid when triggered from the controller's digital signal as shown in **Figure 5.26**. Slightly different from the motor driver diagram in **Figure 5.25**, the resistor connecting the digital input to the gate is of higher resistance because the transistor drew relatively high current, 30mA, from the controller at 100Ω , compared to 3mA at $1k\Omega$. Additionally, a fly-back diode was added due to the properties of a solenoid that prevent it from working without one when connected like this.

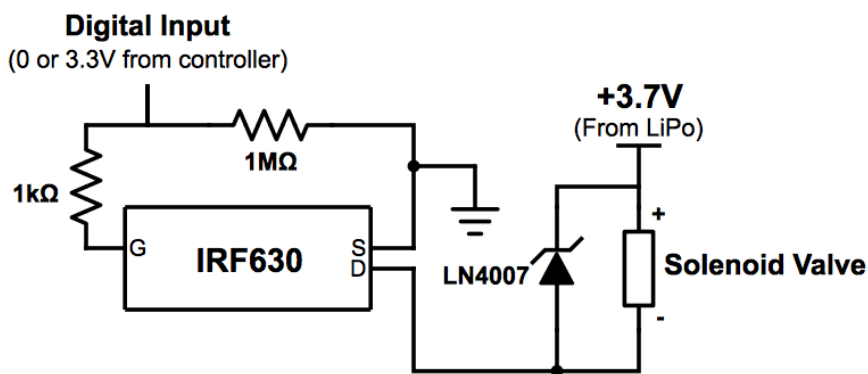


Figure 5.26: Solenoid Pressure Valve Open/Close Circuit

The circuitry for the actuators allowed the vest to inflate and deflate to the standards set at the onset of the project. Moreover, the circuitry for the sensors comprises the other half of the

puzzle that enables these actuators to trigger based on data collected between all of them. The circuitry for almost all of the integrated sensors is extremely simple and unimportant to view in schematic form. The heart rate sensor, noise sensor, and accelerometer were purchased as integrated chips, only requiring a 3.3V differential supplied through the microcontroller and pinning out an output signal. The light sensor and temperature sensor were variable resistors put in series with other resistors to act as a voltage divider. The resistance values were chosen so that the output signals occupied as much of the 0-3.3V range as possible in the potential environments that a child wearing the vest might occupy. However, the circuitry for the air pressure sensor had to be developed.

The air pressure sensor, pictured as a part of the diagram in **Figure 5.27**, provided a near indistinguishable signal between its output pins from its internal Wheatstone configuration when subjected to the pressures within the vest. With the introduction of an LM358 operational amplifying unit, the signal between the output pins of this pressure sensor was differentiated and amplified with a gain of approximately 27. The circuitry for the pressure sensor and its accompanying differential amplification can be seen **Figure 5.27**, and it must be noted that the signal obtained from the vest's internal pressure with the amplification unit was accurate enough to set individualized pressure thresholds and allow the system to operate on a closed feedback loop.

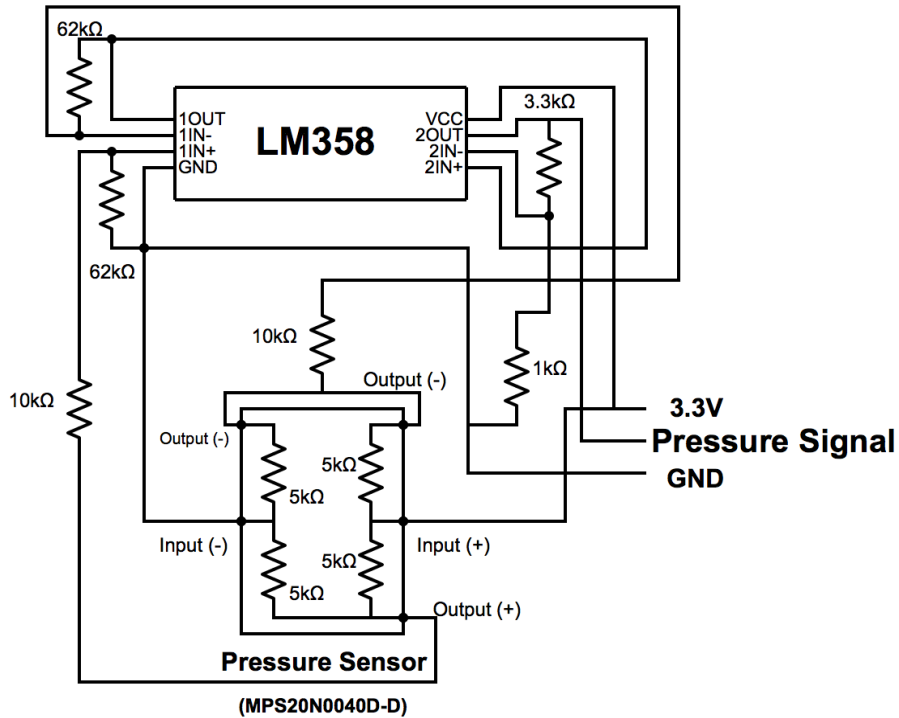


Figure 5.27: Pressure Sensor Differential Amplifier Circuit

Finally, it is important to discuss the placement of all of the circuits, wires, and electrical system components. The microcontroller and battery are placed on the upper portion of the back, centered slightly below the neck because they are the most sizeable components outside of the

pumps and solenoid. The team determined that this location was optimal through comfort testing, discussed further in the **Validation** section. The air pump motor driver circuits are placed adjacent to the pumps by the front of the wearer's hips inside sewn-in pouches because the circuits do not add much space or weight to the predetermined ideal location for the pumps from user comfortability testing. The solenoid and accompanying circuitry is placed adjacent to the pump on the wearer's right side for similar reasons. The sensors are all incorporated on the vest in locations chosen to optimize data collect and minimize obtrusiveness to the user. The heart rate sensor is on the left chest. The light sensor is on the left upper chest area - left vs. right being arbitrary and upper location vital for collecting light sources usually located above children. The sound sensor in the front midsection - midsection being arbitrary and front location vital for collecting noises happening in front of a child though capable of picking up sounds from around a room. The accelerometer and temperature sensor are placed on the back near the controller to consolidate wiring. The internal pressure sensor and circuitry are placed on the upper-middle back for comfort and because the upper portion of the bladders that the sensor is attached to will theoretically be the last area to fill to desired pressure.

5.3.6 Sensor Calibration

All of the sensors feed signals into the microcontroller between 0 and 3.3V. The controls of the system interpreted this data by employing a digital filter over the observed signals so that the system could both respond to and display in the app the current status of all of signals on a rolling basis without inaccurately reporting any unexpected fluctuations in readings. The strength of the filter as well as the measurement of the physical data was calibrated by matching voltage readings against readings of the physical properties of the body and environment. Heart rate is reported in beats per minute, noise in decibels, acceleration in meters per second squared, temperature in degrees of Celsius or Fahrenheit, and pressure in kilopascals. The light sensor was not calibrated to match a physical property such as lumens. Rather, it sensed rapid fluctuations in voltage signal indicating rapid fluctuations in light intensity, a common trigger of sensory overload, so it was decided not to take the time to convert this signal to a property such as lumens because the principle of fluctuation would not change the overall effect on the system. However, in moving the project forward, this would be an easily accomplishable calibration.

The heart rate sensor is calibrated to determine whether the values observed correspond to a peak that is high enough above the filtered voltage signal from the heart rate sensor that it corresponds to an actual heartbeat. The number of beats is then converted to beats per minute based on the time-stamps. The heart rate sensor was calibrated by tweaking the signal filtering constant and the differential voltage between signal and the filtered readings that must be achieved in order for a signal to be considered a beat until the sensor most closely matched readings provided by an Apple Watch. Using this method, the controller is able to perceive heart rate readings within 5 BPM of those being reported by an Apple Watch. The temperature sensor was calibrated by matching the voltage readings against temperatures of various environments indoors and outdoors ranging between 50°F and 80°F until a linear fit was observed between voltages and temperature, yielding an accuracy within about 4°F of the temperature as measured by a thermometer. The noise sensor was calibrated similarly, taken from

environments ranging from 30dB to 80dB until a linear fit was observed from the filtered signal measured against decibel levels reported from a readily available smart phone app, yielding an accuracy within about 3dB of the noise level as measured by a smart phone's microphone. The accelerometer was calibrated against gravity, and the normalized acceleration between the x, y, and z axes of the chip is accurate within about 0.05m/s^2 . Lastly, the internal pressure sensor was calibrated from the pressure supplied by the vest to the torso as discussed in the subsection on **Pressure Distribution Testing**, as opposed to being calibrated from measuring air pressure readings of the bladders while the sensor was operational. Essentially, the internal pressure signals are correlated to the mean pressure supplied to the force sensitive resistors on our child-sized mannequin.

5.3.7 Embedded Software System

While the Feather has a lot of capabilities, it has limits with respect to processing speed (8 MHz) and space (32 kilobytes flash, 8 kilobytes RAM). While the Feather can operate on the Arduino platform, compilation of the standard libraries uses almost one-third of the onboard storage. To free up space and allow for lower-level programming, the HUGS embedded system runs in C++ compiled using a makefile adapted from an open-source [GitHub Repository](#). Utilizing a custom reduced Arduino library, base compilation uses only seven percent of the space on the Feather. This reduced Arduino library can be publicly accessed [here](#).

Due to the aforementioned space and speed constraints, the core processes occur in a single loop, which handles communication, reading/writing, and decision making. If the device is connected to Bluetooth, it reads incoming data then sends its current state. The data is transmitted both ways via a char buffer, with a character indicating the meaning of the following number. Data is only parsed if a character follows the numerical value, meaning that the number was transmitted to completion. These buffers are longer than 20 chars in length (the UART, or Uniform Asynchronous Receiver Transmitter protocol), so only a subset of the values are sent/received on each iteration. The data is therefore staggered between calls, but the device operates quickly enough that all data appears to arrive continuously. The designation of reading versus writing to the BLE communication stream is done using Hayes Commands. After Bluetooth communication, the device reads the analog inputs and determines the current acceleration, noise, light, temperature, and internal pressure readings. It compares these values to the thresholds and determines whether any of the current values should activate the device. This reading is then passed through a low-pass filter tuned to give an approximately 5 second response time to a continuous threshold-exceeding. The desired status is then used in a closed-feedback loop which uses the internal pressure sensor reading to determine whether to activate the pumps, the solenoid, or neither to maintain the desired pressure level.

Additionally, there is a 2 kHz timer used to precisely measure a 5-minute interval for an inflation triggered in proactive mode and to gather readings from the heart rate sensor at a rate of 400 Hz. Due to the lack of space on the Feather, the heart rate algorithm must be online, and due to the nature of interrupts, the algorithm must be efficient. Since no existing algorithms perform well given these constraints, the HUGS device uses a novel algorithm which stores the four previous readings alongside the current and determines if the middle value is a peak. It also

keeps track of a weighted average of the current readings to determine if the magnitude of the peak is significantly far from the average to be the primary pulse in the heart rate rhythm. To eliminate noise from the ambient, there are blocks on jumps in heart rate of significant magnitude. This heart rate reading is then passed into the thresholds in the comparison mentioned in the previous paragraph.

There are two files onboard the microcontroller on the HUGS device: global.h which contains constant definitions, the type definition for the Threshold structure, and static variables and main.cpp which contains the central logic. These files are available publicly [here](#) and are located in the **Appendix, Figures A1 and A2** respectively.

5.3.8 Mobile Application

The HUGS Mobile Application is written in Swift for use in iOS devices. The application features three primary screens, which are shown in storyboard layout in **Figure 5.28** and are detailed below.

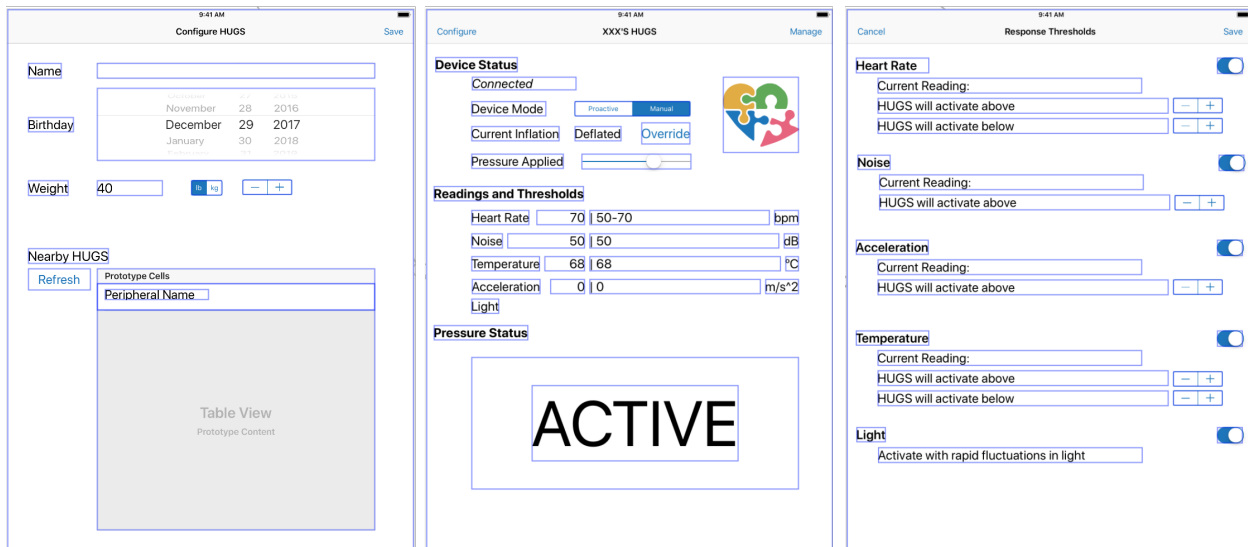


Figure 5.28: HUGS Mobile Application Storyboard

The functionality of the three pages is detailed below in order from left to right.

1. Configurations Page - This page allows the parent/guardian to set the child's name, weight, and birthday. The birthday cannot be set to any date later than the present, and when the units of the weight input change the representation in the label. These variables are passed to the HUGS device when the Save button on the top right of the screen is pressed. Entering this screen also instigates a three-second check for nearby HUGS devices which show up in list form in the bottom half of the screen. This check can be re-started by clicking the "Refresh" button. The application user can connect to the HUGS device by clicking the device name in the list; the device will be highlighted when connected and a blue LED will be enabled on the HUGS garment.

2. Main Landing Page - This page is the primary screen for the device and gives an overview of the connected HUGS device. The top section gives the Device Status: it shows whether or not there is a connected device, and - if connected - allows for the toggle between Manual and Proactive Modes, overrides for inflation/deflation, and a slider to set the desired pressure applied between 5% of the child's body weight and the maximum 19.5%. Setting an override in this section also automatically switches the device into Manual mode, so the override is not undone; this change is made in both the application and onboard the HUGS garment. Since the override has so much capability, there is a pop-up in which the user must confirm the override before it will take effect. The second section of the page shows the last received reading from the HUGS garment of each of the onboard sensors, as well as the thresholds that will trigger activation. The activated thresholds are displayed in black while the deactivated thresholds are gray. The last section shows the pressure application status. The device will read the word "ACTIVE" if the garment is inflating, and the large rectangle will turn yellow. Moving the desired pressure slider sets the height of a nested rectangle with a black outline, and a green rectangle will fill the smaller rectangle as the pressure reaches the desired threshold.
3. Threshold Configuration - This page allows the application user to see the current values from the garment and set the appropriate thresholds for the user. Each threshold can be turned on or off using the toggle to its right, and - if on - the limiting values can be set using the -/+ buttons to the right of that threshold. These changes are not saved until the "Save" button is pressed, and the changes can be undone using the "Cancel" button.

The code for the application is too large for the Appendix of this project (9 files and over 3,000 lines) so it is included in the attached files and can be accessed publicly [here](#). The three screens explained above are in the following three files, in the order in which they were explained above: CreateViewController.swift, MainViewController.swift, and ThresholdViewController.swift. The application handles the Bluetooth communication using Apple's CoreBluetooth protocol, with the mobile application set up as the Core and the device set up as a Peripheral but configured with UartDelegate.swift such that both are capable of receiving and transmitting information. Parser.swift handles the data transmitted in the Bluetooth communication - both parsing the char buffers that are received and configuring the char buffers for writing. The variables global to the application are stored in Global.swift and their values are persistent in the device's memory - meaning that it is possible for the user to close the application, hard quit the application, and restart the device without any loss of the configured values and parameters or data corruption.

5.4 Final System Embodiment and Function of HUGS

The following section details the final system form of HUGS and the way that we envision HUGS being used practically by a child.

5.4.1 Manufactured Final Version

The final HUGS device integrates the mechanical body of the garment with the hardware and software systems discussed above. A combination of permanent stitching, buttons and zippers keep the garment together while allowing for size versatility. This versatility is needed because the intended user is a young child who is constantly growing.

5.4.2 Layers

The mechanical body of hugs is made of three layers. The inner material has been chosen for its comfortability, elasticity and moisture wicking properties. The outer layer was chosen for its stiffness and breathability. The hardware system, comprised of HUGS' five sensors, microcontroller, battery, pumps, solenoid valve, and wiring is sewn directly to the outer layer. The battery and internal pressure sensor circuit board are enveloped in small pouches to ensure comfort for the user by providing a soft interface between the electronics and user, as well as hold the electronics in place despite user motion. Finally, the central bladder system is partially sewn onto the outer material as well. The top portion of the bladders is connected to the outer material with a button to allow for easy access to the microcontroller and battery underneath.

5.4.3 Washability

HUGS is machine-washable, allowing children to live their active lifestyles while receiving the benefits of wearing HUGS every day. The inner layer is detachable from the outer layer via two zippers. One side of each of these zippers is sewn into the outer edges of the inner layer, while the other halves of the zippers are sewn into the inside of the edges of the outer layer of the garment. Thus, the inner layer can be removed and washed. In the current version, the outer layer can only be spot-cleaned because of the sewn-in electronics, but condensing the electronics into a PCB and connecting the rest of the hardware system with removable pouches via buttons or velcro would allow for the both fabrics of HUGS to be machine washable.

5.4.4 Variable Size

Because HUGS is designed for children ages four to six years old, one size does not fit all. The current version is custom designed to fit the child sized mannequin used for pressure distribution testing. If brought to market, two options could be used to achieve variable sizing. The first is that each device would be custom designed to fit the user. This approach is already being used by similar products on the market, namely the T-Jacket [18]. With this approach, three central zippers could be stitched onto the outer layer to allow for the user to continue using HUGS over multiple years as they are growing. The second approach would use large velcro sections rather than zippers to put HUGS on. This approach is used on the market by the Squeeze vest [17]. This would allow for the manufacturer to produce two to three sizes of HUGS, but the user could alter the exact size of their garment to meet their needs with the variable sizing offered by a large velcro section.

6 Validation and Testing

The following sections detail the testing intended and performed on the HUGS device.

6.1 Human Testing

Ideally, testing would be performed on children within the defined user base. Lisa Russell, an Occupational Therapist at the TALK Institute and School in Philadelphia, has extended an offer to test on her patients at the beginning of the year. However, there are FDA requirements that a project must meet in order to test on humans. HUGS may meet the requirements of an exempt study, in which case testing on children may become more feasible [34]. Exempt studies include, “Consumer preference testing, testing of a device modification, or testing of two or more devices in commercial distribution if the testing does not collect safety or effectiveness data, or put subjects at risk.” [35] HUGS could fall under the “device modification” category, as the differences between HUGS and T-Jacket do not significantly change how safe the product is for the user. If HUGS could be considered exempt by the FDA, then the proposed experiment can be submitted for approval by the Penn IRB. Unfortunately, the initial review fee is \$2400, which is the entirety of the provided budget [36], and the IRB approval process timeline is beyond the scope of the project. Therefore, the team was unable to perform response testing on humans.

6.2 Pressure Distribution Testing

It is imperative that deep pressure therapy is applied uniformly around the torso [Appendix Table A1]. Therefore, it was important to test the distribution of pressure applied by the garment.

6.2.1 Pressure Distribution Test Setup

Validation on the pressure applied by the device is performed using a test set-up of twenty Interlink FSR-400 Force Sensitive Resistors on a plastic mannequin approximately the size of a four to six-year old child. The sensors are arranged into four rings of five sensors, each spaced four inches apart along the circumference of the torso of the mannequin. The rings are staggered, so there is a sensor every two inches along the perimeter of the torso, and the rings are separated by a one-inch height differential. The placement of the sensors on the mannequin is shown in **Figure 6.1**.

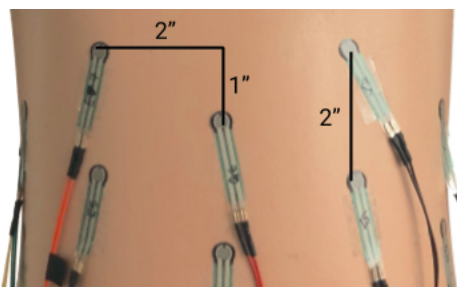


Figure 6.1: Pressure Sensor Spacing on Test Mannequin

The pressure sensing circuitry operates on an Arduino Uno that interfaces with MATLAB. Since there are 20 pressure sensors providing 20 analog values but only six analog ports on the Arduino, the readings are toggled using a multiplexing circuit from two digital pins. The digital output pins are set and toggled in the MATLAB script, with sufficient delays for the circuit to complete without carry-over between states. Internally, the sensors are represented with a character (A-S) for location around the perimeter and a number (4-7) for height in inches from the bottom of the torso. The mux circuit is shown in **Figure 6.2** below.

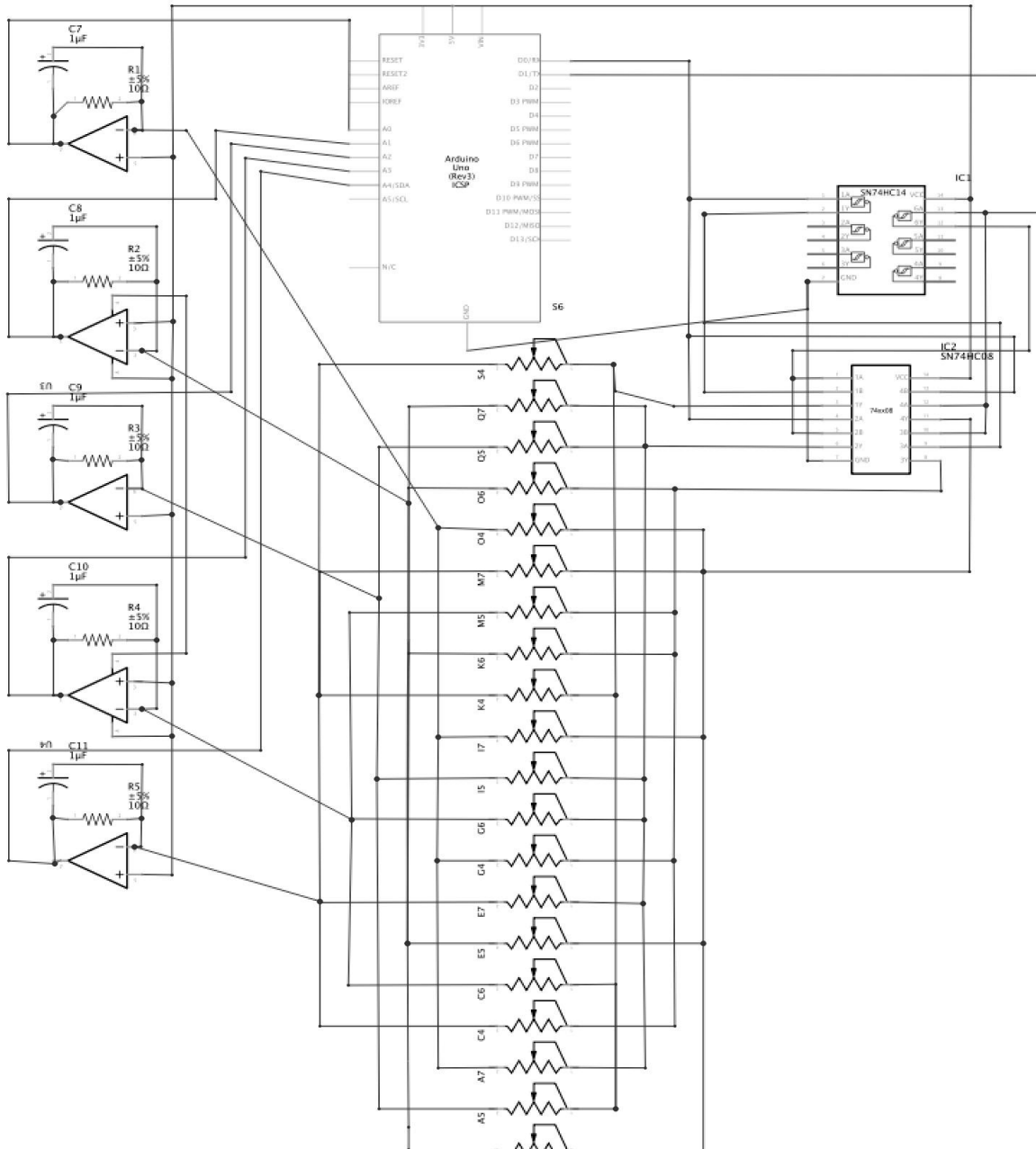


Figure 6.2: Mannequin Pressure Sensor Circuit

The MATLAB script that runs this circuit is included in the **Appendix, Figure A3** and can be accessed publicly [here](#). In the script, each sensor is stored as a PressureSensor object, which converts its two-digit location around the torso into a 3-dimensional point. The pressure values read at these points are then live plotted both in a graph of pressure applied over time and in a 3D elliptical cylinder view which approximates the perimeter of the torso.

The biggest challenge with the pressure testing set up was finding appropriate sensors. There is a physical limitation on the minimum force that can be read by a thin-film force-sensitive resistor of 20 grams force. While there are strain sensors that can operate below this threshold, they require a displacement which means that they would need to extrude from the surface of the mannequin, making them an inaccurate representation of the force applied. Although rated to not read values below 20 grams force, testing the FSR-400 yielded results at around 11 grams force, or about 0.8 kPa. Since HUGS needs to read values in the 1-2 kPa range, these sensors proved sufficient but not optimal. Therefore, in the following tests, the garments were filled to maximum inflation to get the most accurate possible sense of the pressure distribution. By determining the maximum pressure applied and allowing for variable inflation levels below that, both devices are also capable of reaching lower pressures.

6.2.2 Pressure Distribution Results

To analyze the pressure distribution applied by HUGS, the team first looked at the pressure applied by an existing solution. The [Squeeze Jacket](#) is an inflatable deep pressure therapy vest which applies the pressure manually using a pump. The team purchased a Squeeze vest sized for a four to six-year-old child and tested the system on the mannequin with the aforementioned pressure testing configuration. The visual output from the MATLAB Script is included in the **Appendix Figure A4** and a representation of the data is shown below in **Figure 6.3**.

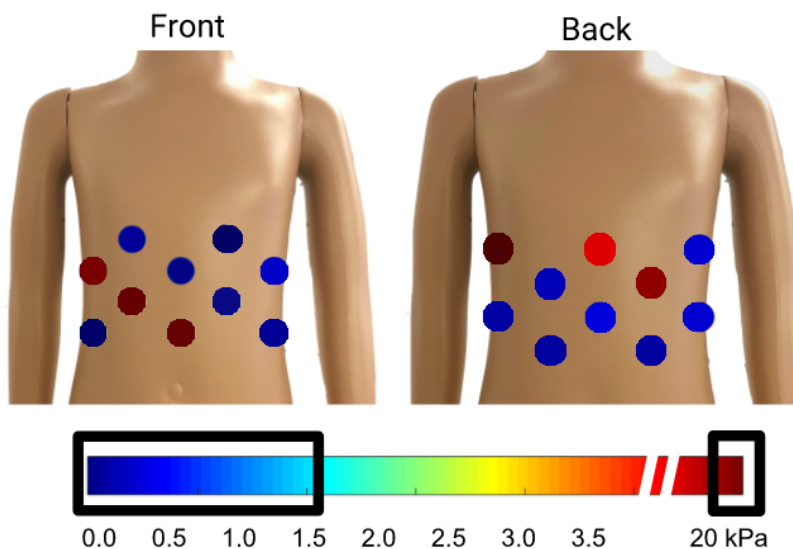


Figure 6.3: Existing Solution Pressure Distribution

As shown above in **Figure 6.3**, the pressure distribution from Squeeze is highly non-uniform with a standard deviation of pressure across the 20 pressure sensors of 7.95 kPa. Comparing this to the HUGS device pressure distribution, we see that HUGS is significantly more uniform and in the range of desired pressures, avoiding extremely high-pressure points like those that Squeeze has.

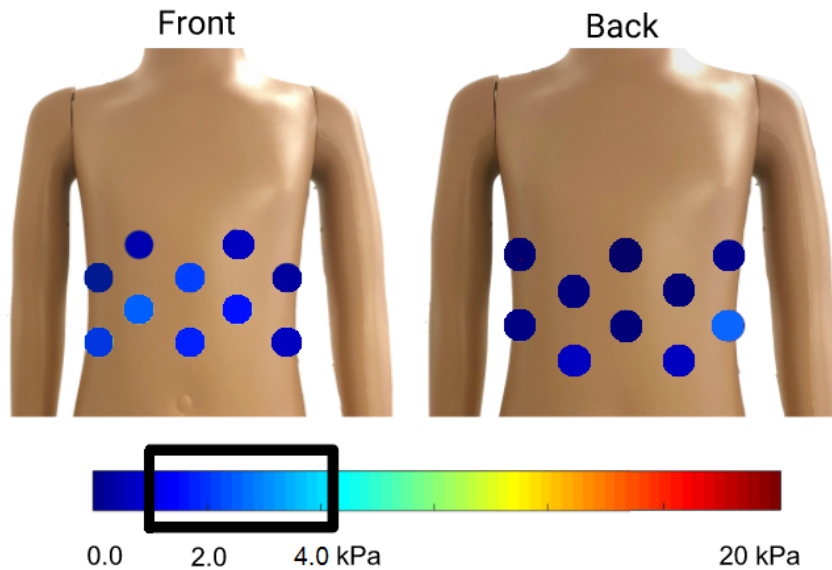


Figure 6.4: HUGS Pressure Distribution

As shown above in **Figure 6.4**, the pressure distribution from HUGS is significantly more uniform with a standard deviation of pressure across the 20 pressure sensors of 1.32 kPa. The MATLAB output from the HUGS device can be found in the **Appendix, Figure A5**.

6.3 Comfort Test

The team performed comfort tests in order to ensure the placement of our pumps and electronics were as comfortable and unnoticeable as possible. We collected quantitative and qualitative feedback make sure that the garment will be comfortable for the child to wear around for the duration of the day with minimal impedance of movement. This includes comfort of the garment overall as well as the comfort of the location of the various subsystems, such as pumps, sensors, and batteries.

We asked participants ($n=15$) to put on the adult sized version of HUGS with all of the electronics attached including the pumps. The electronics and pumps were not wired to the battery in order to ensure there was no accidental inflation of the vest. Next, we asked participants to perform five simple motions (bend forward to touch toes, twist side to side, lean side to side, sit down on a backed chair, and jump up and down three times). We chose these five motions as they reflect common motions a child might use throughout the day, especially in a school environment.

We asked participants to rate the comfort of the vest for each motion on a scale from 1-5, with 1 corresponding to least comfortable and 5 corresponding to most comfortable. Participants were briefed on the 1-5 scale before testing begins. At the end of the test, participants were also asked to rate HUGS' overall comfort, temperature comfort, and movability comfort. Throughout the tests, we took note of the participants' feedback and used both the quantitative and qualitative data to verify the location of our pumps and electronics.

Figure 6.5 below shows the quantitative data gathered during the comfort tests. In each category, HUGS scored above a 3.5 average score. The lowest score was the jumping category, and the consistent feedback we received in this category was that the pumps would swing and hit the user when jumping up and down. In order to remedy this, we switched from a velcro closure mechanism to a zipper, which zipped all the way to the bottom, keeping the pumps close to the body at all times.

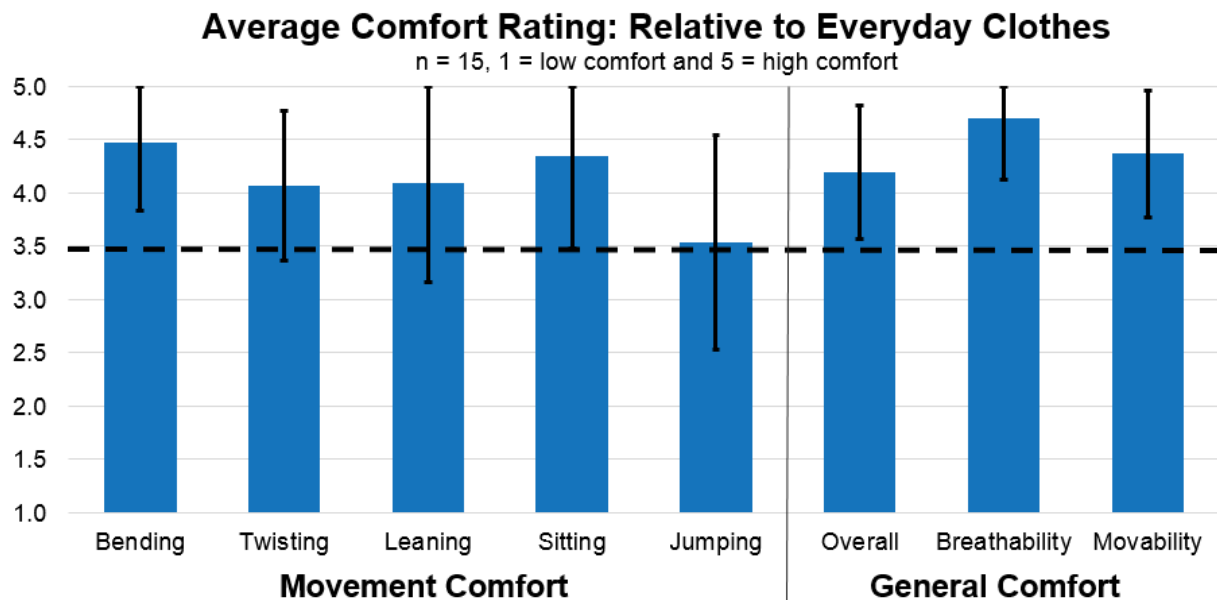


Figure 6.5: Comfort test results

6.4 Sensor Testing

Each of the sensors were tested independently to ensure inflation of the device. The sensors were successful in each of the following tests:

- Accelerometer - The accelerometer was tested by shaking the device both on and off of the mannequin, with only the acceleration threshold enabled. The device activated and began inflation after around 5-6 seconds of shaking. The accelerometer was also tested by letting the garment drop in free-fall, starting from three arbitrary positions. In each of these tests, the garment read out at approximately 1.0 g.
- Noise Sensor - The noise sensor was tested in both quiet and loud environments, with only the noise threshold set, and calibrated to activate approximately 5 dB above the

noise level of the room, as measured by an external decibel meter. The test was performed by recording the status of the device after a few seconds of induced noise: music, talking, singing, white noise, and clapping. The device was successful in 14/15 tests. (Clapping proved ineffective for activation due to the variable noise level. This is something that could be fixed in future iterations.)

- Temperature Sensor - Since the current manufacturing of the bladders is heat based, putting the whole device in a warm environment would have the potential to melt the bladders together, thus making the garment no longer inflatable. Therefore, the temperature sensor was tested by inducing a warm environment in the proximity of the sensor. This was done by bringing a soldering iron close to the garment. With the threshold set at 3°C above the ambient, HUGS activated on all three of these trials.
- Heart Rate Sensor - The heart rate sensor was tested twice - once in calibration and once in an anxiety test. The calibration was performed by comparing the output from the HUGS algorithm to the output produced by a heart rate reading by an Apple Watch. The Apple Watch had surprising fluctuations in values, usually varying on a range of around 15-20 bpm without changes in the user's motion or anxiety level. Over a one-hour period, the HUGS device read consistently within the range set by the Apple Watch fluctuations. The calibration of the device was then confirmed via an anxiety test, in which a member of the team wore the device - calibrated to her resting heart rate - while watching three short scary films. HUGS activated during the climax scene of each of these movies.
- Light Sensor - The light sensors was tested in two configurations - induced increased brightness and induced decreased brightness. The increased brightness test involved flashing a strobe light on the garment and was performed 8 times in rooms of varying brightness. HUGS was successful in inflating in all of these tests. The decreased brightness test was performed by blocking the sensor from the ambient light in an intermittent fashion by waving a hand over the garment repeatedly. HUGS activated every time in five distinct trials.

6.5 Maximum Force Applied

The maximum force applied was tested using the Pressure Distribution Testing setup described above by inflating the bladders to their maximum extent. To achieve this, the pumps were directly connected to a power source and were running continuously at low current until the pressure readings reached a maximum and stabilized. The pressure sensor readings were then averaged, to produce a value of approximately 1.8 g per sensor, or 3.51 kPa.

An average child between the ages of four and six weighs approximately 40 pounds (18 kg) [37] and wears a shirt between a size 4T and a size 6, which have an average length of 42.9 cm and length of 35.5 cm [38]. This means that the average shirt has a surface area of 0.152 m^2 . Assuming that approximately 66% is in contact with the skin and therefore able to have pressure applied, there is an effective surface area of 0.1 m^2 . This is consistent with the test mannequin,

which has a torso surface area of 0.105 m^2 . Therefore, the range for pressure application of 10-15% of a standard child's body weight is 1.78 - 2.67 kPa.

From these calculations, we could determine that the device is capable of reaching maximum pressure of approximately 19.7% of the standard child's body weight. This value is higher than the desired range of 10-15%. Since the device is customizable within that range, the device is therefore operational for children within the target range, as well as more massive children and children who require greater pressure for a response.

6.6 Inflation Time

To test inflation, we pushed remaining air out of the bladders then inflated the bladders to their maximum using the full system configuration and the manual override on the mobile application. The process was timed and repeated five times, each time reaching maximum inflation in 15.8, 15.7, 16.2, 16.8 and 15.4 seconds, therefore averaging around 16 seconds.

6.7 Weight

The mass of the HUGS system was determined by weighing the final system, including all electrical and fabric subcomponents. The total mass of the child's HUGS system is 342 grams.

6.8 Battery Life

The HUGS battery life was analyzed both analytically and through a physical test. The current draw from each component is shown in **Table 5.9** in section 5.3.4 Microcontroller and Battery Selection. Since the solenoid is active for only a few seconds when the bladders need to be deflated, we can assume that there are approximately 30 minutes of total use, meaning that they drain 200 mAh of total battery life, leaving 1800 mAh for the rest of the system. The resulting plot of total battery life as a function of how long the pumps run is shown below in **Figure 6.6**.

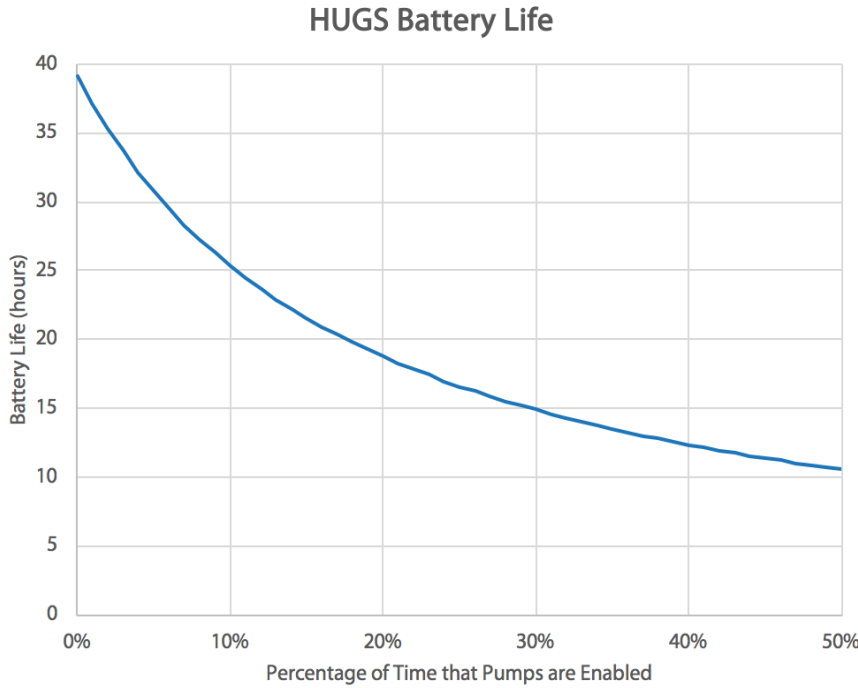


Figure 6.6: HUGS Theoretical Battery Life

Practically, the battery life of HUGS was tested by leaving the device running for a continuous period of time. The device lasted for 14.7 hours; the pumps were actively inflating during 5 of these hours, thus matching the theoretical prediction for around 30%. This surpasses the battery life standards set at the onset of the project.

6.9 Noise at 1m

The noise of the HUGS system was found using a decibel meter in a quiet room (~40 decibels ambient). The decibel meter was placed 1m away from the device and the pumps (the loudest component of the device) were turned on. Over a 20 second period, the decibel meter read continuously around 42 decibels.

6.10 Response Time

Device response time is variable on the continuity of the input given the thresholds. A continuously threshold-exceeding input will thus trigger a response more quickly than something that intermittently surpasses the thresholds, thus making the system less likely to over-predict and over-actuate. The response time was tested repeated on the response of the system to continuous threshold-exceeding input. Over five trials to continuous noise or temperature exceeding inputs, the response time averaged 5.6 seconds.

7 Discussion

The HUGS device meets almost all the goals it set out to achieve. Physical goals such as the uniformity of pressure distribution and maximum force applied have been heavily validated throughout the entirety of the course, and goals relating to the responsiveness of the system, battery life, noise levels, and weight of the system have been met due to careful planning and implementation. Laws and regulations regarding the production of a battery powered, active, wearable device were also of primary focus in the design decision-making process. Though the production of the HUGS device at the culmination of the senior design course has been a success in its own right, there are a variety of things that have the potential to be improved and addressed that could take HUGS from a proof-of-concept prototype to a highly effective proactive wearable device for children with autism that can reduce the truly saddening personal and social impacts of suffering from sensory overload events.

7.1 Target Versus Accomplished Performance

As shown in **Table 7.1**, which is the same as **Table 4.1** with an additional column for final device performance, the HUGS device met all but one of the initial project goals.

Table 7.1: Key Target Specifications vs. Actual Performance of HUGS Device

Objective	Target Specification	Performance
Pressure Distribution	Uniform	Uniform
Max Force Applied	15.0% of body weight	19.5% of body weight
Inflation Time	20 seconds	16 seconds
Response Time	5.0 seconds	5.6 seconds
Battery Life	10 hours	>14 hours
Noise at 1 meter	50 db	42 dB
Weight	<0.80 kg	0.34 kg

Pressure distribution is uniform when measured against the existing deep pressure therapy product Squeeze, as is detailed in the results of the pressure distribution tests discussed in **Section 6.2**. The perceived uniformity of the pressure applied by the HUGS device was also considered and is validated by the touch tests discussed in **Sections 5.2.2.4** and **5.2.2.5**. The maximum force capable of being applied by the vest exceeds the target goal as is discussed in the **Validation** (Section 6.5). Inflation time, battery life, noise at 1 meter, and weight all meet the target specifications largely because pumps were selected that could fill the approximated volume of the child-sized vest based on projected air flow rate, operate at low power

consumption, operate quietly, and were lightweight. Battery selection obviously also was a major factor in battery life. These four performance goals are validated as discussed in **Sections 6.6, 6.8, 6.9, and 6.7** respectively. The only target specification that is technically not met is the response time as discussed by the validation testing in **Section 6.10**. However, the meaning of the response time metric is of considerable interest. When setting out to achieve the fast response time of 5 seconds, the understanding of how the system would operate was more rudimentary. The 5 second response time was established as a means of ensuring the activation of the vest upon sensors reaching binary thresholds—e.g. one's resting heart rate is either above 80 BPM or not and the vest was intended to react within the 5 second response time window if that 80 BPM was set as a threshold for activation and reached. However, the more knowledge obtained regarding how individuals physically show stress from the likes of Dr. Bogen led to the realization that the response window of the device to inputs should be heavily dependent on the individual. So, it is encouraging that the responsiveness of HUGS to sensory input occurs in a time frame close to the target specification, but even though it does not meet the target specification, this target specification is likely more nuanced than originally thought. Methods for addressing this are discussed in the following subsection as a part of the larger discussion of how moving forward with testing on HUGS could aid in the addressing the needs of individuals.

As a wearable consumer product, the HUGS device meets flammability standards, would likely meet the requirements set forth by the Consumer Product Safety Act with minimal adjustments to product architecture, and most importantly, would likely be approved as an FDA General Wellness Product, which would exempt HUGS from a variety of FDA regulations as a low-risk product responsible for reducing the impact of a chronic condition, again, with minimal adjustments to product architecture. Furthermore, HUGS would need to pursue approval from the Federal Communications Commission as a device capable of signal processing between product and smart device. However, this would merely require fulfilling a series of tasks such as obtaining IP addresses for manufactured HUGS devices and verifying communicative performance in a qualified testing facility, so team HUGS is confident in its ability to achieve this approval. Essentially, HUGS either already meets the regulations set forth for wearable consumer products and would simply need to apply for approval or would need to jump through some relatively trivial hoops in the process of applying for approval of the respective governing bodies.

As far as being granted approval for the production and commercialization of an active wearable device designed for children with ASD, the final and most critical regulatory commission HUGS would be responsible for working with and meeting the approval of would be the Institutional Review Board. As mentioned previously in **Section 4.1**, Team HUGS did not seek IRB approval in the construction of the HUGS product for a variety of reasons and declared it to be outside of the scope of the Senior Design project. However, upon the completion of this course, in possession of a highly validated and functional prototype, seeking IRB approval is of the utmost importance in the progression of the HUGS product. Reasoning for this is both obvious and complicated. The necessitation of IRB approval is obvious because of the importance of ensuring the efficacy of the device in mitigating sensory overload events for children with autism. Without this IRB testing approval, it would be impossible to test our product on the

portion of the population that it was intended for. The importance of obtaining IRB approval is more complicated, though, due to the nature of the HUGS device. One would imagine that for many consumer products, IRB approval might be singularly a method for carrying over research and development of a device in order to check for efficacy. However, human testing would be more valuable than a check for efficacy for HUGS; it would actually significantly impact HUGS's development. By collecting biometric and environmental data from children with autism while simultaneously externally monitoring the sensory overload induced behaviors of the children, our team or others continuing to develop the product could implement machine learning mistake-driven algorithms so that HUGS could more effectively respond to the needs of autistic children generally and more effectively respond to the needs of the children on an individual level. The more data collected on the sensory thresholds that most closely indicate sensory overload induced stress or panic for autistic individuals and how these thresholds interact, the smarter the device is capable of being. This will also be addressed further in the following subsection.

7.2 Recommendations

In the development of the HUGS device beyond the realm of MEAM senior design, the most important thing to the value and efficacy of the product revolves around testing the device on autistic children who experience sensory overload and collecting data from their experiences wearing the undergarment.

The first things that would be important to accomplish immediately upon trying to bring the product to market would be to improve the manufacturing methods based on the target market size. This would include consolidating the electronics package into a custom printed circuit board so that excess features on the current microcontroller could be removed and the accelerometer could be integrated into the main data processing chip. Improving manufacturing methods would also require establishing a fabric and electronic assembly method based on the scale of the market size that would be most cost-effective and likely outsourcing air bladder manufacturing. Then, the resulting prototypes ready for full-scale production would be ready to go through tests set forth by the governing bodies discussed briefly in the previous subsection and more in-depth in section 4.1. This would be the next critical step—paying the sums of money necessary to be tested and validated for wireless communication standards, consumer safety standards, and FDA General Wellness Product status.

Finally, the product must go on to obtain IRB approval. As stated, this would consume most of the development effort that would help make the product successful in mitigating sensory overload for Autistic children. Of course, deciding upon scaled manufacturing methods to bring the product to market would require the consultation of a number of professionals, but the intellect and time needed to process large sets of biometric and environmental data would be the most significant aspect of ensuring a high level of success for the product. It would require developing evaluation metrics for product performance such that actuator activity could be compared with the observed sensor data and with the perceived effect of vest activation and deactivation. This dataset could enable the device to operate using Machine Learning

algorithms, in place of the existing threshold comparator. For the device to learn in real-time, it would need to be an online algorithm. One approach would be to use a mistake-driven approach, which would record when an override is performed, along with a feature set including the current sensor inputs, some prior values, and the time of day. This approach would allow the learner to be stored on the mobile application, thus saving space on the system and being individualized to that child. Another approach could be to do generative Machine Learning, which would develop a model of the child's distinct habits and activate given deviations from those habits, thus also becoming unique to the child. With these algorithms, as well as a training set from collected data for feature selection and analysis, the vision for HUGS is to be able to optimally mitigate or completely prevent a sensory overload event.

8 Budget, Donations, and Resources

Table 8.1 below outline the cost of the parts in one HUGS device. At a total cost of \$129.64 using parts purchased at retail cost, we believe that the total cost of parts for HUGS at a production scale would be even lower. Not included in the table are electronic parts provided to us in the GM lab, such as resistors and wires.

Table 8.1: Parts Cost of One HUGS Device

Category	Part	Quantity	Cost Per	Total Cost
Electronics	Adafruit Feather 32u4 Bluefruit LE Microcontroller	1	\$29.95	\$29.95
Electronics	Sound Sensor	1	\$5.95	\$5.95
Electronics	Accelerometer	1	\$9.95	\$9.95
Electronics	Temperature Sensor	1	\$0.75	\$0.75
Electronics	Light Sensor	1	\$0.95	\$0.95
Electronics	Heart Rate Sensor	1	\$24.96	\$24.96
Electronics	DIMINUS DC 6V Mini Air Pump Motor	2	\$4.495	\$8.99
Electronics	3V Mini Solenoid Valve	1	\$3.85	\$3.85
Electronics	Lithium Ion Battery - 3.7v 2000mAh	1	\$12.50	\$12.50
Electronics	Internal Pressure Sensor	1	\$3.50	\$3.50
Fabrics/Inflatables	Mesh Pinnie	1	\$1.50	\$1.50
Fabrics/Inflatables	Under Armour Childs Sports Shirt	1	\$7.50	\$7.50
Fabrics/Inflatables	4 Gauge Vinyl	.25 yards	\$0.75	\$.75
Fabrics/Inflatables	12" Open Ended Zippers	3	\$5.90	\$17.70
Fabrics/Inflatables	PVC Plastic Tubing	.5 feet	\$0.84	\$0.84
TOTAL COST OF PARTS FOR HUGS				\$129.64

Table 8.2 below breaks down the total expenditures on the HUGS project into twelve main categories. We started with a budget of \$2400, and were approved for an additional \$300 in order to purchase a current market solution, Squeeze. We were able to stay under budget, with our expenditures totaling \$1753.07.

Table 8.2: Total Expenditures for Team HUGS

Category	Part(s)	Total Cost
Microcontrollers	Adafruit Feather 32u4 Bluefruit LE	\$131.88
Electronics	Conductive thread, batteries, battery chargers, solenoids	\$194.60
Pumps	6V and 12V pumps	\$35.73
Inflatables	4 gauge Vinyl, PVC tubing, butane soldering iron	\$119.16
Testing	Mannequin, Pressure Sensors	\$294.14
Squeeze	Squeeze Jacket	\$328.90
Materials	Mesh pinnies, kids t-shirts, compression belts	\$85.59
Mechanical Prototype	Motors, axles	\$71.80
Senior Design Day	Pamphlets, stickers, matching shirts/ties	\$159.08+
iPad	iPad for Design day demo	\$240.96
Transportation	Trips for purchasing and meeting Dr. Bogen	\$48.70+
Miscellaneous	Velcro, parchment paper, thermocouple,	\$42.53
Total HUGS Expenditures		\$1753.07

In addition to purchased items, we also utilized the MTS testing machine at the University of Pennsylvania.

9 Intellectual Property

The team was not initially planning on pursuing any Intellectual property, but since design day has reached out to Pam Beatrice and Josh Jeanson at the Penn Center for Innovation to pursue a provisional patent.

The team has conducted a review of patents on similar products as shown in Patents on Similar Products and Designs in the Appendix Table A2.

References

- [1] CDC, "Facts about ASDs," CDC, [Online]. Available: <https://www.cdc.gov/ncbdd/autism/data.html>. [Accessed 25 October 2017].
- [2] T. Field, M. Hernandez-Reif, S. Schanberg and C. Kuhn, "Cortisol decreases and serotonin and dopamine increase following massage therapy," *International Journal Of Neuroscience*, vol. 115, no. 10, pp. 1397-1413, 2005.
- [3] *What it's Like Being Autistic (Sensory Overload) Short Film*. [Film]. National Autism Society, 2016.
- [4] R. Grinker, "Unstrange Minds: Remapping the World of Autism," Basic Books, 2008, pp. 1-11.
- [5] E. J. Marco, L. B. N. Hinkley and S. S. Nagarajan, "Sensory processing in autism: a review of neurophysiologic findings," *Pediatric Research*, vol. 69, no. 5, pp. 48R-54R, 2011.
- [6] J. Coleman, Interviewee, [Interview]. 24 September 2017.
- [7] L. Bestbier and T. I. Williams, "The Immediate Effects of Deep Pressure on Young People with Autism and Severe Intellectual Difficulties: Demonstrating Individual Differences," *Occupational Therapy International*, pp. 1-7, 2017.
- [8] S. M. Edelson, M. G. Edelson, D. C. Kerr and T. Grandin, "Behavioral and physiological effects of deep pressure on children with autism: a pilot study evaluating the efficacy of Grandin's Hug Machine," *American Journal of Occupational Therapy*, vol. 53, no. 2, pp. 145-152, 1999.
- [9] S. Reynolds, S. J. Lane and B. Mullen, "Effects of deep pressure stimulation on physiological arousal," *American Journal Of Occupational Therapy*, vol. 69, no. 3, pp. 1-5, 2015.
- [10] A. M. Colman, "A Dictionary of Psychology (4th edition)," in *A Dictionary of Psychology (4th edition)*, Oxford, Oxford University Press, 2015, pp. 14-15.
- [11] C. Reviews, Thinking About Psychology Mini Book , The Science of Mind and Behavior: Psychology, Psychology, Textbook Reviews, 2016.
- [12] G. De Palo, G. Facchetti, A. Mazzolini, A. Menini, V. Torre and C. Altafini, "Common dynamical features of sensory adaptation in photoreceptors and olfactory sensory neurons," *Scientific Reports*, vol. 3, 2013.
- [13] I. Lampl and Y. Katz, "Neuronal adaptation in the somatosensory system of rodents," *Neuroscience*, vol. 343, pp. 66-76, 2017.
- [14] P. E. Iverson, "Pressure Vest for Treating Autism". United States Patent 20030074711, 24 April 2003.

- [15] "The Bear Hug," Southpaw Enterprises, [Online]. Available: <https://www.southpaw.com/the-bear-hug.html>. [Accessed 26 October 2017].
- [16] "Search Results - SCHOOL SPECIALTY MARKETPLACE," [Online]. Available: https://store.schoolspecialty.com/OA_HTML/xssi_ibSearchResults.jsp?type=search&minisite=10206&query=snug+n+hug. [Accessed 26 October 2017].
- [17] K. d. Greef, "Squease vest | The calming inflatable deep pressure vest," Squeasewear, [Online]. Available: <https://www.squeasewear.com/>. [Accessed 26 October 2017].
- [18] "Non-weighted vest for calming kids with sensory overload, autism, ADHD, sensory processing disorders, PTSD, dementia using deep pressure touch," Tjacket - Non-weighted hug vest that calms children, adults with anxiety, autism, ADHD, SPD, PTSD, [Online]. Available: <http://www.mytjacket.com/>. [Accessed 26 October 2017].
- [19] "Order Snug Vest," [Online]. Available: <https://snug-vest-us.myshopify.com/products/snug-vest>. [Accessed 26 October 2017].
- [20] "Deep pressure | sensory processing | autism | calm | ADHD," Biohug, [Online]. Available: <http://www.biohug.com/>. [Accessed 26 October 2017].
- [21] T. Grandin, "Calming effects of deep touch pressure in patients with autistic disorder, college students, and animals," *Journal of Adolescent Psychopharmacology*, vol. 2, no. 1, pp. 63-72, 1992.
- [22] F. Buckle, D. Franzsen and J. Bester, "The effect of the wearing of weighted vests on the sensory behaviour of learners diagnosed with attention deficit hyperactivity disorder within a school context," *South African Journal of Occupational Therapy*, vol. 41, no. 3, pp. 36-42, 2011.
- [23] "Overcome Anxiety for Good," Anxiety Centre, [Online]. Available: <https://www.anxietycentre.com/>. [Accessed 26 October 2017].
- [24] "Comparative Examples of Noise Levels," IAC Acoustics, 2018. [Online]. Available: <http://www.industrialnoisecontrol.com/comparative-noise-examples.htm>. [Accessed 24 April 2018].
- [25] "Policy for Low Risk Devices," 29 July 2016. [Online]. Available: <https://www.fda.gov/downloads/medicaldevices/deviceregulationandguidance/guidancedocuments/ucm429674.pdf>. [Accessed 25 October 2017].
- [26] "Standard for the Flammability of Vinyl Plastic Film," 2012. [Online]. Available: <https://www.gpo.gov/fdsys/pkg/CFR-2012-title16-vol2/pdf/CFR-2012-title16-vol2-part1611.pdf>. [Accessed 20 April 2018].
- [27] C. P. S. Commission, "CONSUMER PRODUCT SAFETY ACT," 12 August 2011. [Online]. Available: <https://www.cpsc.gov/PageFiles/105435/cpsa.pdf?epslanguage=en>. [Accessed 23 April 2018].
- [28] S. Rossi, "How to get your Bluetooth design FCC and BT certified," January 2017. [Online]. Available:

http://www.st.com/content/ccc/resource/technical/document/application_note/group0/f3/0c/31/34/bf/24/42/89/DM00257329/files/DM00257329.pdf/jcr:content/translations/en.DM00257329.pdf. [Accessed 24 April 2018].

- [29] J.-H. Chen, J.-W. xu and C.-X. Shing, "Decomposition rate of hydrogen peroxide bleaching agents under various chemical and physical conditions," *Journal of Prosthetic Dentistry*, vol. 69, no. 1, pp. 46-48, 1993.
- [30] National Institute for Occupational Safety and Health, "Ammonium Chloride," CDC, 22 July 2015. [Online]. Available: <https://www.cdc.gov/niosh/ipcsneng/neng1051.html>. [Accessed 20 April 2018].
- [31] B. G. Green, "The perception of distance and location for dual tactile pressures," *Perception and Psychophysics*, vol. 31, no. 4, pp. 315-323, 1982.
- [32] M. B. Jones and C. J. Vierck, "Length Discrimination on the Skin," *The American Journal of Psychology*, vol. 86, no. 1, 1973.
- [33] R. Teghtsoonian and M. Teghtsoonian, "Two varieties of perceived length," *Perception and Psychophysics*, vol. 8, no. 6, pp. 389-392, 1970.
- [34] "Medical Device Exemptions 510(k) and GMP Requirements," [Online]. Available: <https://www.accessdata.fda.gov/scripts/cdrh/cfdocs/cfpdc/315.cfm>. [Accessed 24 October 2017].
- [35] U. D. o. H. a. H. Services, "Information Sheet Guidance For IRBs, Clinical Investigators, and Sponsors," January 2006. [Online]. Available: <https://www.fda.gov/downloads/regulatoryinformation/guidances/ucm127067.pdf>. [Accessed 23 October 2017].
- [36] U. o. P. IRB, "IRB Fees | UPENN The Institutional Review Board," 2018. [Online]. Available: <http://www.upenn.edu/IRB/mission-institutional-review-board-irb/irb-fees>. [Accessed 24 October 2017].
- [37] National Center for Health Statistics, "Clinical Growth Charts," 2001. [Online]. Available: https://www.cdc.gov/growthcharts/clinical_charts.htm. [Accessed 23 October 2017].
- [38] "US T-shirt Size, Toddler/Child," [Online]. Available: <http://www.sizechart.com/t-shirt/kids/toddler-children/us/index.html>. [Accessed 25 October 2017].

Appendix

Summary of Feedback from Experts

Table A1: Summary of Occupational Therapist Responses

Expert Name	Position/Title	Use DPT?	Uniform vs. Gradient?	Continuous vs. Intermittent?
Venus David	occupational therapist and Founder of So Love Autistic Center	Uses weighted vests and a roller DPT system (similar to hug machine)	n/a	"It doesn't work continuously; after desensitization, it's no longer effective at all"
Lisa Russell	occupational therapist at TALK Institute and School	Uses weighted vests and hug machines	Noted that her patients prefer pressure to be fairly uniform and over as large an area as possible	Only uses weighted vests for short time periods (10-15 minutes) due to desensitization
Roseann Schaff	occupational therapist at Jefferson Hospital	"We have seen that it does help children [with ASD] calm down a bit and decrease their sensory reactivity...and arousal"	n/a	n/a
Dr. Trenna Sutcliffe	Medical Director at Sutcliffe Developmental and Behavioral Pediatrics Clinic	"Kids with autism, ADHD, or trouble with self regulation or anxiety in general could benefit from [a garment] that could increase compression in moments of stress."	n/a	For a "sensory diet" she recommends 5-10 minutes of pressure every 2-3 hours, with certain exceptions of up to ~20 minutes for recess or more unstructured time

Brittany Johansen	occupational therapist (recently moved practice to CA)	"There are interventions with equipment, such as compression clothing - such as compression shirts, and also vests that we use that provide that deep pressure input."	n/a	n/a
Sarah Bujno	Staff at residential group home for children with developmental disabilities	Used weighted vests and blankets with children at the group home	"My concern is that it will provide too little/too much/uneven pressure, exacerbating the crisis"	n/a

Microcontroller Source Code

global.h

```

#pragma once
#define LIGHT_ALPHA 0.9
#define INF_ALPHA 0.1
#define INF_PUMP_THRESHOLD 0.9
#define INF_SOLENOID_THRESHOLD 0.3
#define PRESSURE_THRESHOLD_MULTIPLIER 1.2
#define PUMP_PIN1 5
#define PUMP_PIN2 13
#define PRESSURE_ATM 150
#define SOLENOID_PIN 10

struct Threshold {
    bool isOn;
    float upperBound;
    float lowerBound;
};

static double HR_ALPHA = 0.95;
static uint16_t incr = 0;
static uint16_t averageHRInput = 0;
static uint16_t currHR = 80;
static float currNoise = 50.0;
static int8_t currTemp = 60;
static float currAccel = 1.0;
static float currLight = 300.0;
static float averageLight = 5.0;
static float currIntPressure = 0;

static Threshold hrThresh;
static Threshold noiseThresh;
static Threshold accelThresh;
static Threshold tempThresh;
static Threshold lightThresh;

static bool isProactive = false;
static bool shouldInflate = false; // only used in manual mode

```

```

static float weight;

static bool inflating = false;
static float inflationValue = 0.0;
static uint32_t inflationCountdown = 0;
static uint16_t prev0HR = 0;
static uint16_t prev1HR = 0;
static uint16_t prev2HR = 0;
static uint16_t prev3HR = 0;
static uint16_t prev4HR = 0;
static uint16_t prevT = 0;

```

Figure A1: Source Code for Embedded System Static, Global Constants

main.cpp

```

#include <Arduino.h>
#include <SPI.h>
#include "Adafruit_BLE.h"
#include "Adafruit_BluefruitLE_SPI.h"
#include "BluefruitConfig.h"
#include "global.h"

#define HUGS_GARMENT 0
// 1: adult
// 0: baby

void writeValuesToBLE();
void readValuesFromBLE();
void parseInput(String str);
void parseTULthreshold(Threshold* th, String str);
void parseTLthreshold(Threshold* th, String str);
void parseTthreshold(Threshold* th, String str);
void parseSettings(String str);
void readAnalogInputs();
void readTimedAnalogInputs();
void calculateLight();
uint8_t determineState();
void setDigitalOutputs();

Adafruit_BluefruitLE_SPI ble(BLUEFRUIT_SPI_CS, BLUEFRUIT_SPI_IRQ, BLUEFRUIT_SPI_RST);
float desiredPressure = PRESSURE_ATM + 10;

void setup(void) {
    ble.begin(VERBOSE_MODE);
    ble.echo(false);
    ble.verbose(false);
    if (HUGS_GARMENT == 1) {
        ble.sendCommandCheckOK(F("AT+GAPDEVNAME=ADULT_HUGS"));
    }
    if (HUGS_GARMENT == 0) {
        ble.sendCommandCheckOK(F("AT+GAPDEVNAME=CHILD_HUGS"));
        digitalWrite(12, LOW);
        digitalWrite(11, LOW);
        digitalWrite(9, LOW);
    }
}

cli();
TCCR0A = 0;
TCCR0B = 0;
TCNT0 = 0;
OCR0A = 255; // 2kHz
TCCR0A |= (1 << WGM01);
TCCR0B |= (1 << CS01) | (1 << CS00);
TIMSK0 |= (1 << OCIE0A);
sei();

pinMode(PUMP_PIN1, OUTPUT);
pinMode(PUMP_PIN2, OUTPUT);
pinMode(SOLENOID_PIN, OUTPUT);
pinMode(A0, INPUT);
pinMode(A1, INPUT);
pinMode(A2, INPUT);
pinMode(A3, INPUT);

```

```

pinMode(A4, INPUT);
pinMode(A5, INPUT);
pinMode(A7, INPUT);
pinMode(A9, INPUT);
}

void loop(void) {
    if (ble.isConnected()) {
        writeValuesToBLE();
        ble.waitForOK();
        readValuesFromBLE();
    }
    readAnalogInputs();
    inflationValue = inflationValue * (1-INF_ALPHA) + determineState() * INF_ALPHA;

    if (!isProactive) {
        inflating = shouldInflate;
        inflationCountdown = 0;
    } else {
        if (inflationCountdown == 0) {
            inflating = (inflationValue > INF_PUMP_THRESHOLD);
            if (inflating) { inflationCountdown = 150000; }
        }
    }
    setDigitalOutputs();
}

ISR(TIMER0_COMPA_vect){
    incr++;
    if (incr % 5 == 0) {
        readTimedAnalogInputs();
    }
    if (inflationCountdown > 0) { inflationCountdown--; }
}

void readValuesFromBLE() {
    ble.println("AT+BLEUARTRX");
    ble.readline();
    if (strcmp(ble.buffer, "OK") == 0) { return; }
    parseInput(ble.buffer);
    ble.waitForOK();
}

void writeValuesToBLE() {
    ble.print(F("AT+BLEUARTTX="));
    ble.print('h');
    ble.print(currHR);
    ble.print('\n');
    ble.print(currNoise);
    ble.print('t');
    ble.print(currTemp);
    ble.print('a');
    ble.print(currAccel);
    ble.print('c');
    ble.print(currIntPressure - PRESSURE_ATM);
    ble.print('i');
    ble.println(inflating ? 1 : 0);
}

void readAnalogInputs() {
    float x = (analogRead(A0)-511.0)/102.0;
    float y = (analogRead(A1)-511.0)/103.0;
    float z = (analogRead(A2)-517.0)/102.0;
    currAccel = abs(pow(x*x+y*y+z*z,0.5) - 1.0);
    currNoise = 0.75 * currNoise + 0.25 * (abs(int(analogRead(A3))-511.0) * 0.488 + 62.514);
    currLight = analogRead(A5);
    averageLight = LIGHT_ALPHA * averageLight + (1.0-LIGHT_ALPHA) * currLight;
    currTemp = int8_t(-0.107382*analogRead(A9)+98.8);
    currIntPressure = analogRead(A7);
}

void readTimedAnalogInputs() {
    prev4HR = prev3HR;
    prev3HR = prev2HR;
    prev2HR = prev1HR;
    prev1HR = prev0HR;
    prev0HR = analogRead(A4);
}

```

```

averageHRInput = averageHRInput * 0.995 + prev0HR * 0.005;
if (prev2HR > averageHRInput + 80 && prev1HR > prev0HR && prev2HR > prev1HR && prev2HR > prev3HR &&
    prev3HR > prev4HR) {
    uint16_t deltaT = incr > prevT ? incr - prevT: uint32_t(incr - prevT + 65535);
    uint16_t tempHR = (60.0 / (deltaT/1000.0));
    if (tempHR > currHR - 30 && tempHR < currHR + 30) {
        currHR = round(currHR * HR_ALPHA + tempHR * (1.0-HR_ALPHA));
        prevT = incr;
    }
}

void setDigitalOutputs() {
    if (inflating) {
        if (currIntPressure > desiredPressure * PRESSURE_THRESHOLD_MULTIPLIER) {
            // deflate
            digitalWrite(SOLENOID_PIN, HIGH);
            digitalWrite(PUMP_PIN1, LOW);
            digitalWrite(PUMP_PIN2, LOW);
        } else if (inflating && currIntPressure < desiredPressure) {
            // inflate
            digitalWrite(SOLENOID_PIN, LOW);
            digitalWrite(PUMP_PIN1, HIGH);
            digitalWrite(PUMP_PIN2, HIGH);
        } else {
            // hold pressure
            digitalWrite(SOLENOID_PIN, LOW);
            digitalWrite(PUMP_PIN1, LOW);
            digitalWrite(PUMP_PIN2, LOW);
        }
    } else {
        if (currIntPressure < PRESSURE_ATM) {
            // deflate
            digitalWrite(SOLENOID_PIN, HIGH);
            digitalWrite(PUMP_PIN1, LOW);
            digitalWrite(PUMP_PIN2, LOW);
        } else {
            // hold pressure
            digitalWrite(SOLENOID_PIN, LOW);
            digitalWrite(PUMP_PIN1, LOW);
            digitalWrite(PUMP_PIN2, LOW);
        }
    }
}

void parseInput(String str) {
    switch(str[0]) {
        case 'h': parseTULthreshold(&hrThresh, str); break;
        case 't': parseTULthreshold(&tempThresh, str); break;
        case 'n': parseTLthreshold(&noiseThresh, str); break;
        case 'a': parseTLthreshold(&accelThresh, str); break;
        case 'l': parseTthreshold(&lightThresh, str); break;
        case 's': parseSettings(str); break;
    }
}

uint8_t determineState() {
    return ((hrThresh.isOn && (currHR > hrThresh.upperBound || currHR < hrThresh.lowerBound)) ||
            (tempThresh.isOn && (currTemp > tempThresh.upperBound || currTemp < tempThresh.lowerBound)) ||
            (noiseThresh.isOn && (currNoise > noiseThresh.upperBound)) ||
            (accelThresh.isOn && (currAccel > accelThresh.upperBound)) ||
            (lightThresh.isOn && (abs(currLight - averageLight) > 50.0)));
}

void parseTULthreshold(Threshold* th, String str) {
    if (str.length() >= 3) { th->isOn = (str[2] == '1'); }
    uint8_t index = 4;
    String boundString = "";
    while (index < str.length() && str[index] != ',') {
        boundString += str[index];
        index++;
    }
    th->lowerBound = boundString.toDouble();
    index++;
    boundString = "";
    while (index < str.length() && str[index] != '\n') {
        boundString += str[index];
        index++;
    }
    th->upperBound = boundString.toDouble();
}

```

```

}

void parseTLthreshold(Threshold* th, String str) {
    if (str.length() >= 3) { th->isOn = (str[2] == '1'); }
    uint8_t index = 4;
    String boundString = "";
    while (index < str.length() && str[index] != '\n') {
        boundString += str[index];
        index++;
    }
    th->upperBound = boundString.toDouble();
}

void parseTthreshold(Threshold* th, String str) {
    if (str.length() >= 3) { th->isOn = (str[2] == '1'); }
}

void parseSettings(String str) {
    if (str.length() >= 3) { isProactive = (str[2] == '1'); }
    if (str.length() >= 5) { shouldInflate = (str[4] == '1'); }
    uint8_t index = 6;
    String string = "";
    while (index < str.length() && str[index] != ',') {
        string += str[index];
        index++;
    }
    weight = string.toDouble();
    index++;
    string = "";
    while (index < str.length() && str[index] != '\n') {
        string += str[index];
        index++;
    }
    desiredPressure = PRESSURE_ATM + 50 * max(string.toDouble(), 0.1);
}

```

Figure A2: Source Code for Embedded System Logic

Pressure Distribution Testing Source Code

PressureSensor.m

```

classdef PressureSensor
properties
    radialVal
    x
    y
    z
end
methods
    function obj = PressureSensor(letter, height)
        obj.radialVal = double(uint8(letter) - 65);
        obj.z = height;
        theta = deg2rad(18*obj.radialVal);
        r = 3.5*2.75/(sqrt((2.75*cos(theta))^2+(3.5*sin(theta))^2));
        obj.x = r*cos(theta);
        obj.y = r*sin(theta);
    end
end
methods (Static)
    function dist = getDistance(obj, r2, theta2, z)
        dTheta = mod(abs(theta2 - obj.theta), 180);
        arcLength = dTheta * (r2 + obj.r)/2;
        dist = arcLength^2 + (z-obj.z)^2;
    end
    function name = getName(obj)
        name = sprintf('%s%d', char(obj.radialVal+65), obj.z);
    end
end
end

```

Figure A3a: Source Code For PressureSensor Object in Pressure Testing Software

pressureMap.m

```
clear;clc;clf, close all
import PressureSensor

%% Define Sensors
K5 = PressureSensor('K', 5);
G5 = PressureSensor('G', 5);
C5 = PressureSensor('C', 5);
O5 = PressureSensor('O', 5);
S5 = PressureSensor('S', 5);
E6 = PressureSensor('E', 6);
M6 = PressureSensor('M', 6);
I6 = PressureSensor('I', 6);
A6 = PressureSensor('A', 6);
Q6 = PressureSensor('Q', 6);
K3 = PressureSensor('K', 3);
G3 = PressureSensor('G', 3);
C3 = PressureSensor('C', 3);
O3 = PressureSensor('O', 3);
S3 = PressureSensor('S', 3);
E4 = PressureSensor('E', 4);
M4 = PressureSensor('M', 4);
I4 = PressureSensor('I', 4);
A4 = PressureSensor('A', 4);
Q4 = PressureSensor('Q', 4);

%% Define States
states = [[K5 S5 A6 E4 S3];
           [G5 E6 Q6 I4 C3];
           [C5 M6 Q4 M4 G3];
           [O5 I6 A4 O3 K3];];

%% Gather Pressure Readings from the Sensors
ard = arduino('COM5', 'uno', 'Libraries', 'Servo');
configurePin(ard, 'A0', 'AnalogInput');
configurePin(ard, 'A1', 'AnalogInput');
configurePin(ard, 'A2', 'AnalogInput');
configurePin(ard, 'A3', 'AnalogInput');
configurePin(ard, 'A4', 'AnalogInput');
configurePin(ard, 'A5', 'AnalogInput');
configurePin(ard, 'D3', 'pullup');
configurePin(ard, 'D4', 'pullup');
configurePin(ard, 'D3', 'DigitalOutput');
configurePin(ard, 'D4', 'DigitalOutput');
ardInd = ['A0'; 'A1'; 'A2'; 'A3'; 'A4'; 'A5'];

%% Create Cylinder
[Xcyl, Ycyl, Zcyl] = cylinder(2.75);
Xcyl = Xcyl * 3.5/2.75;
Zcyl = Zcyl*4 + 3;

%% Set Graph Parameter
[numStates, sensorsPer] = size(states);
numVals = numStates * sensorsPer;
valsToPlot = 20;
pauseTime = 0.5;
xData = zeros(1, numVals);
yData = zeros(1, numVals);
zData = zeros(1, numVals);
cData = zeros(1, numVals);
for state = 1:numStates
    for sensor = 1:sensorsPer
        index = sensor+(state-1)*sensorsPer;
        xData(index) = states(state, sensor).x;
        yData(index) = states(state, sensor).y;
        zData(index) = states(state, sensor).z;
    end
end
figure('Color','w')
axis vis3d
subplot(1,2,1)
hold on
surf(Xcyl, Ycyl, Zcyl, 'FaceColor', 'k', 'FaceAlpha', 0.2);
s = scatter3([], [], [], 100, [], 'filled');
colorbar
```

```

colormap(jet)
caxis([0 20])
set(s, 'XData', xData, 'YData', yData, 'ZData', zData);
title('3D Visualization of Torso Pressure Distribution (kPa)')
axis off

subplot(1,2,2)
ts = 0:pauseTime:(valsToPlot-1)*pauseTime;
values = zeros(numVals, valsToPlot);
title('Pressure Reading By Sensor Over Time')
ylabel('Pressure Sensed (kPa)')
xlabel('Time (s)')
axis([0 valsToPlot*pauseTime 0 20])
hold on
legend('show');
plots = [plot(ts, zeros(numVals,1), 'Color', [.4 0 0], 'DisplayName', PressureSensor.getName(states(1,1)));
plot(ts, zeros(numVals,1), 'Color', [.7 0 0], 'DisplayName', PressureSensor.getName(states(1,2)));
plot(ts, zeros(numVals,1), 'Color', [1 0 0], 'DisplayName', PressureSensor.getName(states(1,3)));
plot(ts, zeros(numVals,1), 'Color', [1.5 0], 'DisplayName', PressureSensor.getName(states(1,4)));
plot(ts, zeros(numVals,1), 'Color', [1 .7 0], 'DisplayName', PressureSensor.getName(states(1,5)));
plot(ts, zeros(numVals,1), 'Color', [1 1 0], 'DisplayName', PressureSensor.getName(states(2,1)));
plot(ts, zeros(numVals,1), 'Color', [0 .7 0], 'DisplayName', PressureSensor.getName(states(2,2)));
plot(ts, zeros(numVals,1), 'Color', [0 .5 0], 'DisplayName', PressureSensor.getName(states(2,3)));
plot(ts, zeros(numVals,1), 'Color', [0 .5 1], 'DisplayName', PressureSensor.getName(states(2,4)));
plot(ts, zeros(numVals,1), 'Color', [0 .7 1], 'DisplayName', PressureSensor.getName(states(2,5)));
plot(ts, zeros(numVals,1), 'Color', [0 0 1], 'DisplayName', PressureSensor.getName(states(3,1)));
plot(ts, zeros(numVals,1), 'Color', [0 0 .7], 'DisplayName', PressureSensor.getName(states(3,2)));
plot(ts, zeros(numVals,1), 'Color', [0 0 .5], 'DisplayName', PressureSensor.getName(states(3,3)));
plot(ts, zeros(numVals,1), 'Color', [.5 0 .5], 'DisplayName', PressureSensor.getName(states(3,4)));
plot(ts, zeros(numVals,1), 'Color', [.7 0 .7], 'DisplayName', PressureSensor.getName(states(3,5)));
plot(ts, zeros(numVals,1), 'Color', [.1 0 .1], 'DisplayName', PressureSensor.getName(states(4,1)));
plot(ts, zeros(numVals,1), 'Color', [.3 .3 .3], 'DisplayName', PressureSensor.getName(states(4,2)));
plot(ts, zeros(numVals,1), 'Color', [.5 .5 .5], 'DisplayName', PressureSensor.getName(states(4,3)));
plot(ts, zeros(numVals,1), 'Color', [.7 .7 .7], 'DisplayName', PressureSensor.getName(states(4,4)));
plot(ts, zeros(numVals,1), 'Color', [0 0 0], 'DisplayName', PressureSensor.getName(states(4,5))]];
hold off

%% Gather Data
ind = 1;
while true
    ind = max(1, mod(ind, 21));
    for state = 0:numStates-1
        %Configure Output Pins for State
        writeDigitalPin(ard, 'D3', mod(state, 2));
        writeDigitalPin(ard, 'D4', state > 1);
        for i = 1:numStates
            for j = 1:sensorsPer
                index = j + (i-1)*sensorsPer;
                set(plots(index), 'YData', values(index,:));
            end
        end
        %Update from sensor reading
        for sensor = 1:sensorsPer
            index = sensor + state*sensorsPer;
            cData(index) = (readVoltage(ard, ardInd(sensor,:)) * 143)/(50.27)*9.8;
            values(index, ind) = cData(index);
        end
    end
    ind = ind + 1;
    set(s, 'CData', cData);
    mean(cData)
    drawnow
end

```

Figure A3b: Pressure Sensing Setup Collection, Mux, and Graphics Source Code

Pressure Distribution MATLAB Outputs

Squeeze Jacket

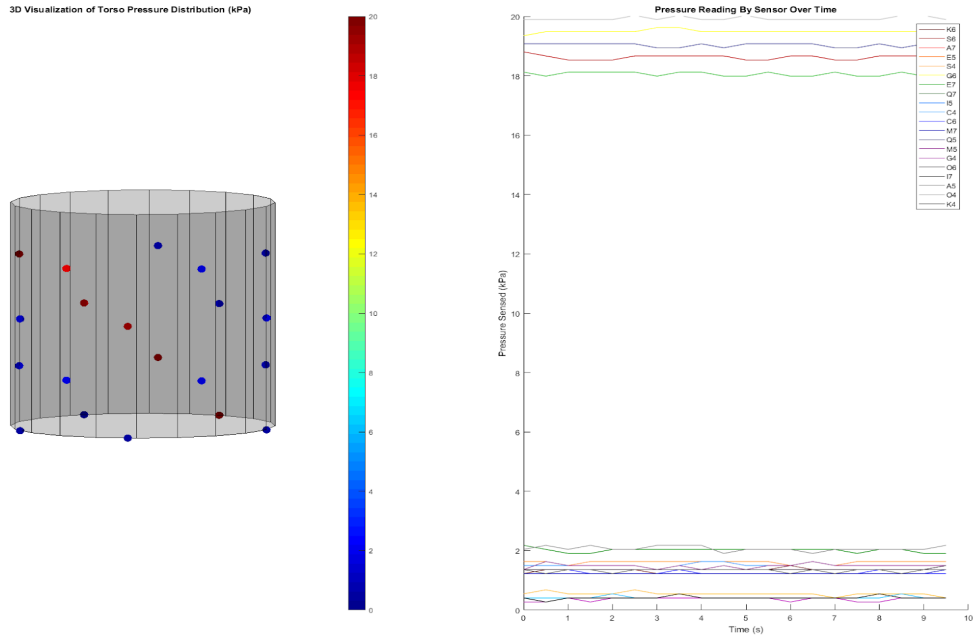


Figure A4: Squeeze Jacket Pressure Distribution

HUGS

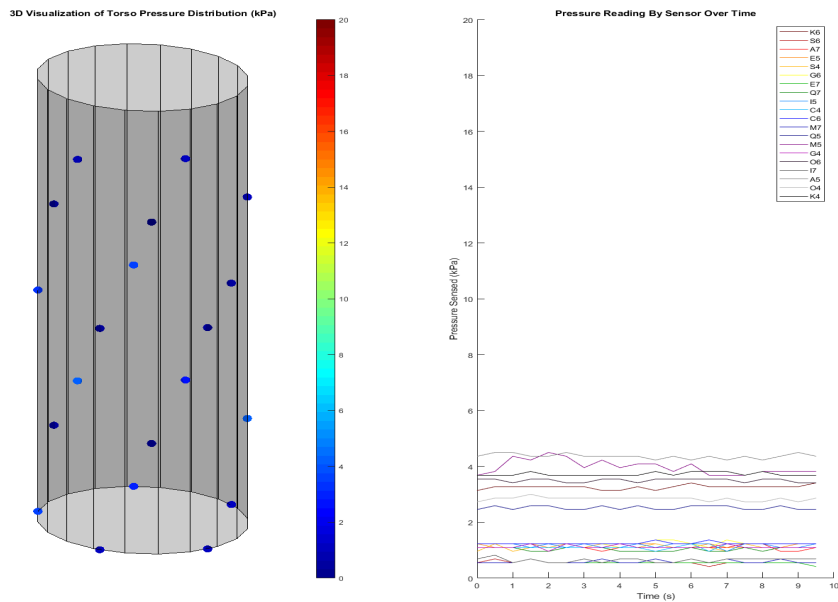


Figure A5: HUGS Pressure Distribution

Patents on Similar Products and Designs

Table A2: Relevant Patent Summary

Patent	Filing Date	Publication Date	Applicant	Title
US5454376	8/16/1993	10/3/1995	Stephens; David L.	Breathing monitor articles of wearing apparel
US6757916	8/28/2002	7/6/2004	Mustang Survival Corp.	Pressure applying garment
US20040040064	8/28/2002	3/4/2004	Donald Mah	Pressure applying garment
EP1871329A2	3/27/2006	1/2/2008	Carmel-Haifa University Economic Corp. Ltd.	Wearable soothing system
EP1871329A4	3/27/2006	12/29/2010	Carmel Haifa University Economic Corp Ltd	Wearable soothing system
US7618384	9/20/2006	11/17/2009	Tyco Healthcare Group Lp	Compression device, system and method of use
US20080071202	9/20/2006	3/20/2008	Tyco Healthcare Group Lp	Compression Device, System and Method of Use
US20080086064	9/28/2007	4/10/2008	Carmel - Haifa University Economic Corporation Ltd.	System and method for reducing and/or preventing anxiety in individuals
US20090177130	12/7/2007	7/9/2009	Wegher-Thompson Seth M	Deep pressure methods, apparatus and systems for autism therapy and other therapies
US20080125684	2/7/2008	5/29/2008	Tyco Healthcare Group Lp	Disposable band for a compression device
US20100010404	9/21/2009	1/14/2010	Tyco Healthcare Group Lp	Self-contained compression device with spring-biased housing members and method
US20100010405	9/21/2009	1/14/2010	Tyco Healthcare Group Lp	Self-contained compression device with pneumatic bladder and method
US20100010406	9/21/2009	1/14/2010	Tyco Healthcare Group Lp	Self-contained compression device with cam-movable housing members and method
WO2012046068A1	10/6/2011	4/12/2012	Squeeze Ltd	Garment with inflatable bladders for application of therapeutic pressure

US943353 2	11/27/2012	9/6/2016	Covidien Lp	Tubeless compression device
US880164 3	1/10/2013	8/12/2014	Covidien Lp	Compression garment assembly
US952685 9	1/31/2013	12/27/2016	Biohug Technologies, Ltd.	Device method and system for reducing anxiety in an individual
US201600 01034	1/31/2013	1/7/2016	Biohug Technologies Ltd.	Device method and system for reducing anxiety in an individual
WO201311 4370A1	1/31/2013	8/8/2013	Biohug Technologies, Ltd	Device system and method for reducing anxiety in an individual
WO201412 0094A1	1/30/2014	8/7/2014	Lai Sep Riang	A garment for treating sensory disorder

Rayleigh Number and Perceived Heat MatLab Code

```
%%
clc;clear
%Plot Rayleigh Number of gap as function of bladder spacing

%Input properties of air
alpha = 2.2536*10^-5; %Thermal diffusivity in m^2/s
beta = 3.2933*10^-3; %Thermal expansion coefficient in 1/K
nu = 1.8704*10^-5; %Dynamic viscosity in kg/m*s
Tq = 296; %Ambient temp in K
Tp = 307; %Person temp in K
g = 9.81; %acceleration due to gravity in m/s^2
k = .026378; %Thermal conductivity in W/mK

%Create symbolic variable for length characteristic and equation
% syms H
% assume(H>0 & H<0.0258);

H = 0.013:0.001:0.026;

RaG = g*beta*(Tp-Tq)*H.^3/(nu*alpha);

%Plot Rayleigh number
figure
% subplot(2,1,1)
plot(H,RaG,'b','LineWidth',2)
hold on
plot([0 0.026], [1708 1708],'r','LineWidth',2)
plot([0 0.026], [2562 2562],'k','LineWidth',2)
xlabel('Gap Between Air Bladders (m)', 'FontSize',14)
ylabel('Rayleigh Number', 'FontSize',14)
title('Bladder Geometry Optimization', 'FontSize',14)
xlim([.013 .026])
legend({'Rayleigh Number', 'Lowest Allowable Rayleigh Number', 'Target Rayleigh Number'},'Location','northwest','FontSize',14)
% plot(.0129,2285,'ko') %reference value of bladders
hold off

%%
%Find h of gap as function of bladder spacing

%Calculate dimensionless parameters
Pr = nu/alpha;
NuG = 0.18*(Pr*RaG/(Pr+0.2)).^0.29;

%Calculate Hydraulic Diameter
L = 0.0129;
```

```

PG = 2*L+2.*H;
AcG = L.*H;
DG = 4*AcG/PG;

%Find h
hg = NuG*k/L;

%%
%Find h of bladders

%Calculate dimensionless parameters
RaB = 2284.7;
NuB = 0.18*(Pr*RaB/(Pr+0.2))^0.29;

%Calcualte Hydraulic Diameter
w = 0.0254;
PB = 2*L+2*w;
AcB = L*w;
DB = 4*AcB/PB;

%Find h
hb = NuB*k/L;

%%
%Find Thermal Resistance

%Surface Areas/Cross Sectional Areas
Ab = 0.0254*0.508; %area of bladder touching body
Ag = H.*0.508; %area of gap touching body
SAb=(2*0.0254*0.508)+(2*.0129*.508); %area of convection for bladder
SAg=(2*.0129*.508); %area of convection for gap
Rt = 1./(1./(hg.*SAg))+(1/(hb*SAb)));
% Rt = 1./Rt;
%% Find Resistance of Fabrics
kv=.155; % thermal conductivity of vinyl (W/mK)
kfabric=.04; % thermal conductivity of fabric (W/mK)
Lv=.0001; %thickness of vinyl (m)
Lfab=.0006; %thickness of fabric(m)

Rv=Lv/(kv*Ab); %resistance of vinyl
Rg=Lfab./(kfabric.*(Ab+Ag)); %resistance of fabric

Rtotal=Rt+Rv+Rg;
%%
%Plot Temperature of person
q = 280; %Heat flux of a person
A = (SAb+SAg);
Tperson = (q.*A.*Rtotal)+Tq;
TpersonC = Tperson - 273.15;
TpersonF = TpersonC*9/5 +32;
Hcm=H.*100;
TdiffC=TpersonC-33;
TdiffF=TpersonF-91.4;
zeroline=zeros(size(Hcm));
% subplot(2,1,2)
% hold on
plot(Hcm,Tdiff,'r')
%plot(Hcm,zeroline,'k')
xlabel('Gap Between Air Bladders (cm)', 'FontSize', 14)
ylabel('Deviation from Normal Torso Temperature (?C)')
%ylim([0,1.8])

```

Figure A6: Rayleigh Number and Perceived Heat MatLab Code

Heat Transfer MatLab Code

```

%% Plane Wall Approximation
% This version assumes a plane wall. We can use it to approximate heat
% transfer per unit length [m] across the prototype. This essentially
% assumes that the torso is flat. We can also create a cylindrical wall
% approximation if desired.

clc
clear
close all

```

```

% Variables
i = .001; % [m] thickness of inner matl
o = .001; % [m] thickness of outer matl
b = .001; % [m] thickness of bladder matl
a = .01; % [m] thickness of air bladder
g = .1; % [m] height of gap bn bladders
h = .6; % [m] height of one bladder
d = 1; % [m] unit length across the prototype ie 'depth' into page of cross section

k_i = .26; % thermal conductivity of inner matl (0.26 W/m-K from COMSOL lib)
%k_o = .05; % thermal conductivity of outer matl ()
k_b = .1; % thermal conductivity of bladder matl (0.1 W/m-K from COMSOL lib)
k_air = .02624; % thermal conductivity of air in bladder (for dry air at 300K W/m-K)
%h_air = .05; % conv heat transfer coeff for air in bladder
h_amb = 5; % conv heat transfer coeff bn outer matl and ambient air (free conv standard)

Ttorso = 305; %(90 -32)*(5/9) + 273.15; % [K]
TambientF = [0:150];
TambientC = (TambientF -32).*(5/9);
Tambient = (TambientF -32).*(5/9) + 273.15; % [K]
deltaT = Ttorso - Tambient; % [K]

% Thermal Resistances
Rinner = i / (k_i * (2*h + g) * d);
Router = 0; %o / (k_o * h * d);
R2air = a / (k_air * (2*h + g) * d); % if conduction
%R2air = 1 / (h_air * H * d); % if convection
R1b = b / (k_b * h * d);
R1air = b / (k_air * g * d); % if conduction
% R1air = 1 / (h_air * (H-(2*h)) * d); % if convection
R3b = b / (k_b * h * d);
R3air = b / (k_air * g * d); % if conduction
% R3air = 1 / (h_air * (H-(2*h)) * d); % if convection
Rconv = 1 / (h_amb * (2*h + g) * d); % convection bn outer matl and ambient air

% Analyses
Rtotal = Rinner + ( (2/R1b) + (1/R1air) )^(-1) + R2air + ( (2/(R3b + Router)) + (1/R3air) )^(-1) + Rconv;

qtotal = deltaT ./ Rtotal./(2*h + g); % [W/m^2]

% Plot
graph = plot(Tambient, qtotal, 'color', [21/325 116/325 188/325], 'LineWidth',3);
grid off
%title('Total Heat Transferred from Body to Ambient','FontSize',24)
%title('Heat Out of Torso [W/m^2]', 'FontSize',20)
xlabel('Ambient Temp [K]', 'FontSize',32)
ylabel('Heat Out of Torso [W/m^2]', 'FontSize',32)
axis([290 299 10 25])
set(gca, 'FontSize',18);
hold on
plot(Tambient(69),qtotal(69),'.k','MarkerSize',50)
%matchT = '\leftarrow T_{ambient} = 20^{\circ}\text{C}';
%matchq = 'q_{out} = 20 \text{ W/m}^2';
%matchx = 20+3;
%matchy = qtotal(69)+2;
%text(matchx,matchy,matchT,'FontSize',26)
%text(matchx,matchy-15,matchq,'FontSize',26)

```

Figure A7: Heat Transfer MatLab Code